Technical feasibility assessment for hydrogen transport through existing offshore gas pipelines in the Dutch sector

by

H.S.Hillen

to obtain the degree of Master of Science in Offshore & Dredging Engineering,

at the Delft University of Technology,

to be defended publicly on Monday February 25, 2019 at 14:00 PM.

Student number:	4189450	
Thesis committee:	Prof. dr. A.V. Metrikine,	Delft University of Technology
	Dr. ir. A. Jarquin Laguna,	Delft University of Technology
	Ir. P. Swart,	Shell
	Ir. R. Vulla,	Nederlandse Aardolie Maatschappij
	Dr. ir. A.H.M. Krom,	NV Nederlandse Gasunie
	Dr. ir. A.J. Bottger,	Delft University of Technology

This thesis is confidential

Abstract

In the last century, the offshore industry has installed a network of offshore pipelines in the southern North Sea. Due to decreasing oil and gas extraction in the North Sea, many pipelines of this network are becoming redundant. A potential option for the reuse of these pipelines is the transport and storage of gaseous hydrogen, which is increasingly considered as an attractive energy carrier for a fossil fuel free economy. A Shell study has shown that offshore hydrogen production located at a renewable energy source, such as an offshore wind park, can economically compete with onshore hydrogen production that uses power cables to transport the energy to shore. The offshore hydrogen production case is based on newly built pipelines. If it is technically feasible to use existing pipelines, this can contribute to making the offshore hydrogen production case more attractive.

A transition from hydrocarbon transport to hydrogen transport through existing carbon steel gas pipelines changes the material behaviour of the pipeline, including a change in fatigue behaviour. Fatigue damage due to Vortex-induced vibrations (VIV) in offshore pipeline parts that are suspended above the seabed is a major challenge for oil and gas transportation in the southern North Sea. Therefore, it is of great importance to understand the change in fatigue behaviour due to the presence of gaseous hydrogen to assess the technical feasibility of hydrogen transport through the existing offshore pipelines.

A fatigue analysis for a specified existing gas pipeline in the southern North Sea has been done according to DNV Free Spanning Assessment Methodology. For this analysis, the fatigue SN-curve for carbon steel material in a hydrogen environment is required. The SN-curve is approached based on available fatigue data for carbon steel material in hydrogen and severe sour environments. It shows that hydrogen has a significant influence on the fatigue behaviour of carbon steel material. The fatigue analysis outcomes show that adjustments to the pipeline are needed to avoid a significant increase in the risk of fatigue failure in critical pipeline sections. A remediation analysis has shown that rock dumping comes out as the cheapest option.

An existing time-domain numerical model that can determine the dynamic behaviour of a pipeline due to VIV is extended to perform fatigue damage calculations. The pipeline is modelled as a Euler-Bernoulli beam using the Finite Element Method. The model determines the VIV with a modal analysis in time-domain, which allows the model to include non-linear soil behaviour. The fatigue damage is determined for each pipeline element, which gives the fatigue damage distribution over the length of the pipeline. The time-domain numerical model is compared with the DNV Free Spanning Assessment Methodology and gives significantly higher fatigue lives. This suggests that the methodology that is used for the fatigue analysis is too conservative. However, there is still uncertainty about the influence of parameters predicting VIV. Further calibration of the model is required to ensure that the model outcomes correspond with target failure probabilities regarding industry standards.

The general conclusion of this research is that the specified existing offshore gas pipeline is technically suitable for the transport of hydrogen if the adjustments are conducted. Compared to newly built pipelines, hydrogen transport through existing pipelines is an attractive option due to relatively low adjustments costs.

Preface

This thesis is written to obtain the degree of Master of Science in Offshore and Dredging Engineering at the Delft University of Technology. The research is commissioned by Shell at their location in Rijswijk.

The thesis report would not have been possible without the support of many people. First of all, I would like to say that I am very grateful to ir. Pieter Swart (Shell) for making it possible to do this graduation project at Shell and for his supervision, support and enthusiasm about the subject. I also want to thank prof. dr. Andrei Metrikine (TU Delft) for being the chair of my graduation committee, and my university supervisor dr. ir. Antonio Jarquin Laguna (TU Delft) for all his help along the way. Also, I want to thank Ir. J.M. de Oliveira Barbosa (TU Delft) for his support with the modelling. I also appreciate the willingness of dr. ir. Alfons Krom (Gasunie) for sharing his knowledge about the effect of hydrogen on materials. Furthermore, I want to give a special thank to Sze Yu Ang (Shell) and Morten Slingsby, who assisted me with the programs that I used in this research. Finally, I want to thank Bostjan Bezensek (Shell) and Raju Vulla (Shell) for their involvement in the project.

Contents

Nomenclature

Nomenclature

$[K_{element}]$	Stiffness matrix of the element	–
$[T_{Element}]$	Tangent stiffness matrix of the element	–
$[U_{dynamic}]$	Dynamic deflections and rotations factor	–
$[U_{static}]$	Static deflection and rotation vector	–
α_e	Temperature expansion coefficient	$\frac{1}{^\circ C}$
ΔK	Cyclic stress intensity range	$Pa\sqrt{m}$
Δp_i	Pressure difference relative to laying	Pa
ΔT	Temperature difference relative to laying	$^\circ C$
$\Delta\omega$	Stress range	Pa
$\Delta\sigma$	stress range	Pa
λ_m	Normal stress	Pa
θ	Angle	rad
A_c	Material cross-section area	m^2
A_i	Internal cross-section area	m^2
c	Crack length	m
D	Outer diameter	m
d	Fatigue damage	–
E	Young's modulus	Pa
f_n	Natural frequency	s^{-1}
f_v	Vibration frequency	s^{-1}
f_{crit}	Critical frequency	s^{-1}
H_{eff}	Effective lay tension	N
I	Inertia	m^4
KDF_{Esat}	Saturated knockdown factor	–
$KDF_{hydrogen}$	Knockdown factor for hydrogen environment	–
KDF_{sour}	Knockdown factor for sour environment	–
M	Moment	Nm
M_y	Moment in y-direction	Nm

M_z	Moment in z-direction	Nm
n	Number of cycles	$-$
n_f	Number of cycles to failure	$-$
pH	Acid value	$-$
pH_2S	Partial pressure	Pa
r	Outer radius	m
St	Strouhal number	$-$
$Seff$	Effective axial force	N
u	Deflection	m
V	Near-seabed current velocity	m/s
v	Kinematic viscosity	m^2/s
V_r	Reduced velocity	$-$

Chapter 1

Introduction

1.1 Background

In the last century, the offshore industry has installed a network of offshore pipelines in the southern North Sea. These existing pipelines are used for the transportation of oil and gas between several offshore platforms and from these platforms to shore. Due to decreasing oil and gas extraction in the North Sea, pipelines of this pipeline network are becoming redundant. Therefore, the question arises if these pipelines can be reused for other purposes.

A potential option for the reuse of redundant pipelines in the southern North Sea is the transport and storage of gaseous hydrogen. Currently, hydrogen is receiving an increasing amount of attention as it is considered as an attractive energy carrier for a fossil fuel free economy [1]. In such an economy, hydrogen can be introduced as an energy carrier for offshore renewable energy projects. In this concept, a hydrogen production plant is placed on an offshore platform alongside a renewable energy source, such as an offshore wind park. This offshore hydrogen production plant contains an electrolyser that generates gaseous hydrogen from renewable energy and water, as displayed in figure 1.1. Thereafter, the generated hydrogen will be transported through the pipelines to shore. The production of hydrogen will have zero emissions. Therefore, hydrogen is considered as a green energy carrier although recent research have shown that the leakage of hydrogen during production and transportation could have an effect on global warming [2]. OH-radicals in the atmosphere that are able to break down methane can react with hydrogen. Therefore, the OH-radicals are not available to break down methane. However, the effect on the environment of the leakage of hydrogen is minimal in comparison with the leakage of hydrocarbons during hydrocarbon transport.

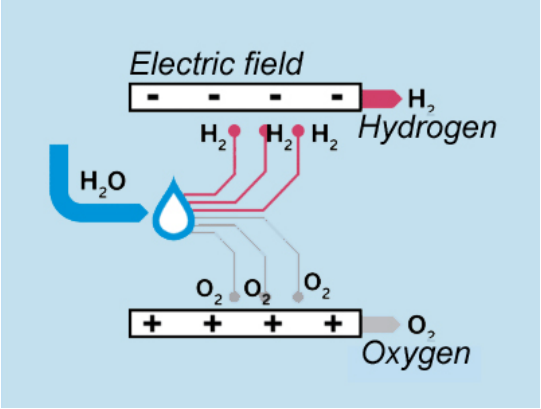

FIGURE 1.1: Electrolysis [3]

Shell has conducted a financial study to investigate the potential of hydrogen in offshore wind energy projects [4]. This study has shown that offshore hydrogen production can economically compete with onshore hydrogen production that uses power cables to transport the energy to shore. The main difference in the cost-structure between both cases are the costs of the energy export system that transport the energy to shore. The offshore case makes use of pipelines, while the onshore case makes use of more costly power cables. The Shell study states that offshore hydrogen generation becomes economically interesting when either the capacity of the renewable energy source crosses a threshold value or when the distance of the plant to the coast exceeds a certain distance. The offshore hydrogen production case is based on newly built pipelines. If it is technically feasible to use existing pipelines, evidently this will make the offshore hydrogen production case more attractive.

Besides cost-efficiency, an advantage of energy transport with hydrogen as the energy carrier compared to electrical transmission is that it is easier to store the energy of the hydrogen molecules in pipelines or reservoirs than to store the electric power in expensive batteries.

To investigate the potential of hydrogen transport through offshore pipelines, it is essential to understand the effects of hydrogen on the mechanical properties of the pipeline, and to examine the potential hazard before a safe implementation in the energy system could be ensured. This applies to all assets of the energy system including offshore pipelines. The Norwegian gas transport operator Gassco studied the feasibility of hydrogen transport through existing offshore gas pipelines [5]. Their study included the pipeline integrity, pipeline integrity management, safety and environmental impact. Based on their research, they concluded that there were no clear show-stoppers identified. However, the effect of hydrogen embrittlement and the change in fatigue behaviour were the main unresolved issues and required further research. Therefore, this research focuses on the effect of hydrogen embritllement and the change in fatigue behaviour to assess the technical feasibility of hydrogen transport through existing carbon steel pipelines, and the pipelines in the Southern North Sea in particular.

1.2 Problem description

A transition from hydrocarbon transport to hydrogen transport through existing carbon steel gas pipelines leads to changes in the material behaviour of the pipeline's steel. In particular, the presence of hydrogen could potentially lead to hydrogen embrittlement. This embrittlement degrades steel performance including a change in fatigue behaviour of the material.

Fatigue damage due to Vortex-induced vibration (VIV) in exposed offshore pipelines is a major challenge for the transportation of oil and natural gas in the southern North Sea. The southern North Sea has a continually changing seabed topology that leads to the formation of freespans along offshore pipelines. Freespans are parts of the pipeline that are not supported by the seabed. Vortex-induced vibrations could occur in freespans when pipelines are subjected to near-seabed currents, which are the main source of fatigue damage. Fatigue could lead to rupture of the pipeline. Based on available empirical fatigue data, it is expected that the transition from hydrocarbons transport to hydrogen transport will lead to an increased probability of fatigue failure.

1.3 Research objective

The objective of this research is to assess the technical feasibility of transporting hydrogen through offshore gas pipelines in the Dutch sector. The potential of an existing offshore gas pipeline will be evaluated as part of a potential future value chain. To investigate this objective, the following main research question in formulated:

What is the technical feasibility of transporting hydrogen through offshore gas pipelines in the southern North Sea?

To investigate this main research question, the following research sub-questions have been formulated:

- What is the change in material behaviour of carbon steel pipelines due to the transition from hydrocarbon transport to hydrogen transport?
- What is the fatigue behaviour of carbon steel pipelines for hydrogen transport in comparison with hydrocarbon transport?
- Which adjustments need to be made to be able to transport hydrogen through carbon steel pipelines for the next 30 years in a safe way and how is this done economically?
- What is the difference in the fatigue damage results between a time-domain numerical model and the DNV Free Spanning Assessment Methodology (DNV-RP-F105)?

The answers to these research sub questions will lead to the main conclusion of this research.

1.4 Project scope

This thesis focuses on pipelines in the southern North Sea. The pipelines are made of different types of high strength carbon steel material and the pipelines have their own specifications in terms of site-specific metocean data and freespan formation. This research will focus on one specified pipeline.

For the technical feasibility of hydrogen transport through existing offshore gas pipelines, all components that may come into contact with hydrogen must be able to withstand the negative effects of hydrogen. However, this research will only focus on the horizontal part of the pipeline on the seabed, as shown in figure 1.2. Therefore, the valves and the compressors are beyond the scope of this research.

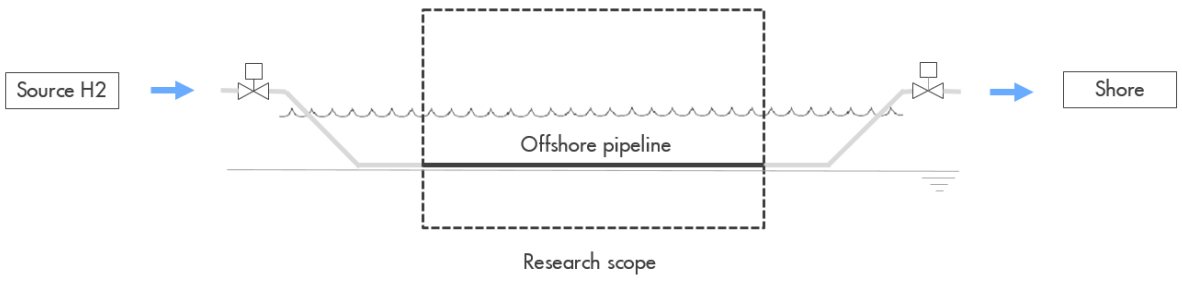

FIGURE 1.2: Project scope

The horizontal part of the pipeline includes the girth welds that are applied during installation. These girth welds are the weakest spots of the pipeline. Therefore, it is assumed that a girth weld is always located at the highest stress location of the entire freespan length.

Before the implementation of hydrogen transport through the pipeline, safety needs to be ensured. The safety depends on the risk, which can be described by the probability of an event times the consequences of this event. This research focuses on the increase in probability that pipeline failure occurs for the transition to hydrogen transport.

Lastly, this research assumes 100 percent clean dry hydrogen, which will be transported in the gas phase at room temperature.

1.5 Research method

This section outlines the steps that are conducted in this research. A framework of the research method is displayed in figure 1.3.

1 Creation of an overview of the theoretical background that is needed to assess the technical feasibility of hydrogen transport through carbon steel pipelines, based on a desk study and interviews with industry experts.

2 Data collection for the pipeline . This data includes fatigue test data, site-specific metocean data, pipeline properties and freespan historical data.

3 Derivation of a theoretical method to estimate a fatigue curve for carbon steel in a hydrogen environment based on limited available fatigue test data.

4 Familiarisation with the DNV modelling program Fatfree which is an Excel sheet based on DNV Free Spanning Assessment Methodology (DNV-RP-F105) that can do a fatigue analysis for offshore freespan, and the execution of a fatigue analysis for the specified pipeline.

5 Familiarisation with a time-domain numerical model developed in the thesis "Dynamic Interaction of Subsea Pipeline Spans due to Vortex-induced Vibrations" [6] that can do determine the dynamic behaviour due to VIV of offshore freespans. Extend the time-domain numerical model to be able to perform fatigue damage calculations.

6 Conducting a fatigue analysis for the pipeline.

7 Run several case studies to compare to the outcomes of Fatfree with the outcome of the time-domain numerical model for freespans.

8 Probability analysis for the formation of critical freespans to identify the pipeline sections which a high probability on the formation of critical freespans, based on pipeline historical data and a sediment migration analysis.

9 Remediation analysis to determine the most suitable adjustment to avoid an increase of the probability of failure in critical freespans in the pipeline.

10 Summarise the conclusions of this research and give a recommendation for future research.

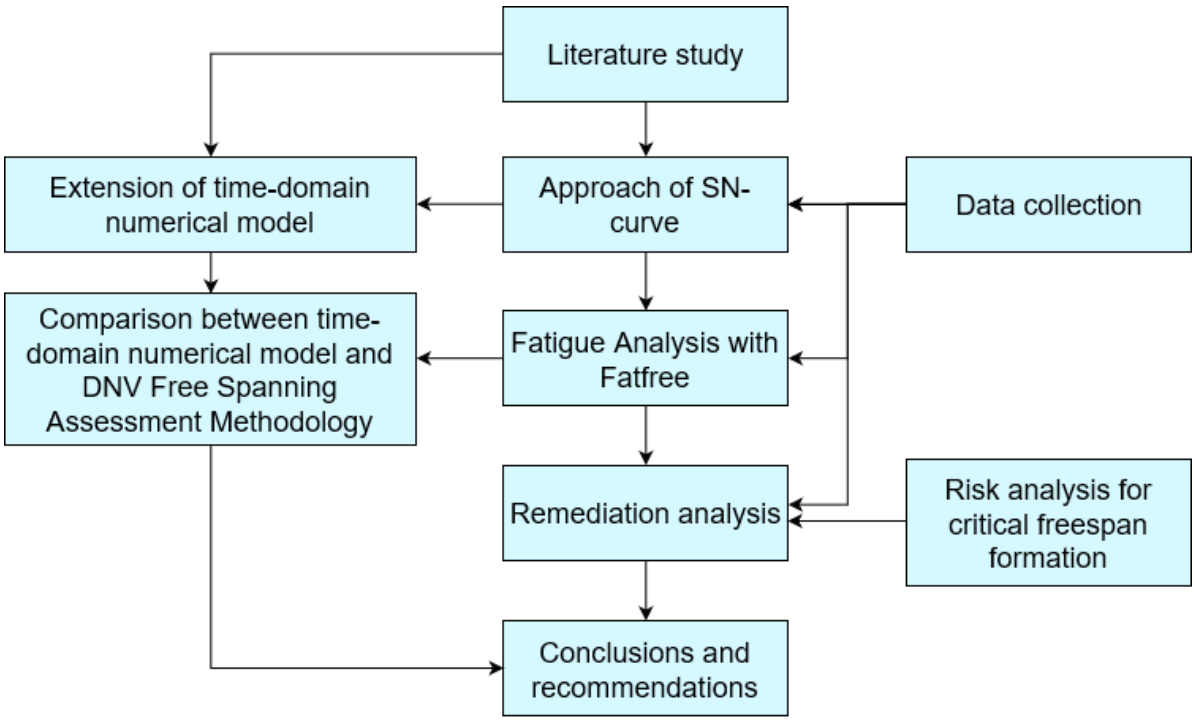

FIGURE 1.3: Framework of the research method

1.6 Research outline

The remainder of this research is organised in the following structure. To get a good understanding of the background theory of this research and to find the literature gaps, an overview of the theory is given in chapter 2. In order to be able to determine the fatigue behaviour in the pipeline, a theoretical method is developed to approach a fatigue curve for a material in a hydrogen environment with limited available fatigue test data. This method and the approach of the fatigue curve for carbon steel material in a hydrogen environment are described in chapter 3. Chapter 4 introduces the characteristics of the specified pipeline. Also, an overview of the fatigue analysis of the pipeline is presented in chapter 4 that is done with the DNV freespan modelling program Fatfree. Chapter 5 discuss which adjustments are possible to avoid an increased probability of failure due to the transition to hydrogen transport through the specified pipeline. A time-domain numerical model for freespans is created in MATLAB to examine the conservatism of the results of the fatigue analysis in Fatfree. Chapter 6 explains the construction of this MATLAB model, and discuss the differences in outcomes between both programs. Chapter 7 summarise the conclusions of this research and present the recommendations for future work.

Chapter 2

Theory

This chapter gives an overview of the theoretical background that is needed to assess the technical feasibility of hydrogen transport through the pipeline, and it identifies the gaps in the literature. Section 2.1 discusses the change in material behaviour due to the presence of hydrogen. After that, the risks of these changes in material behaviour for a pipeline in an offshore environment is addressed. The rest of this chapter is about fatigue behaviour. Vortex-induced vibrations (VIV) have a prominent role in the fatigue behaviour in offshore pipelines. Therefore, section 2.2 extensively elaborates on the theory about these vibrations. This section also discusses the stresses in the pipelines due to VIV. Section 2.3 addresses the theory about fatigue and the probability of failure for offshore pipelines are discussed. Also, the change in fatigue behaviour due to the presence of hydrogen is discussed.

2.1 Change in material behaviour due to atomic hydrogen

Corrosion of carbon steel pipelines due to the presence of a relatively small amount of wet hydrogen sulphide, H_2S, in the pipeline is a common problem in the oil and gas industry. In the presence of water, the hydrogen sulphide molecules could split into H^+ and HS^-. H^+ ions can react to molecular gaseous hydrogen, H_2, or penetrate the pipeline's material [7]. Atomic sulphide, S^{2-}, that occurs when HS^- splits, slows the recombination of the atomic hydrogen into molecular hydrogen. Therefore, the presence of atomic sulphide will drastically accelerate the penetration rate of atomic hydrogen into the material [8].

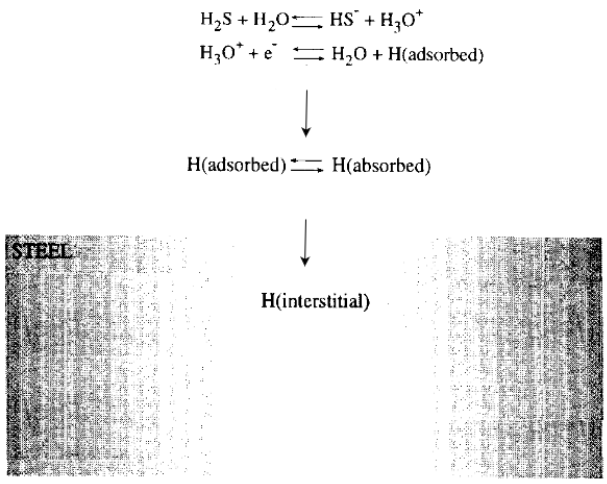

FIGURE 2.1: Illustration of the penetration of atomic hydrogen in carbon steel for a severe sour environment [7].

Hydrogen transport through the pipeline will lead to a similar process. Hydrogen molecules could dissociate in hydrogen atoms. The atomic hydrogen can recombine to molecular hydrogen or can penetrate the pipeline's material at a clean surface.

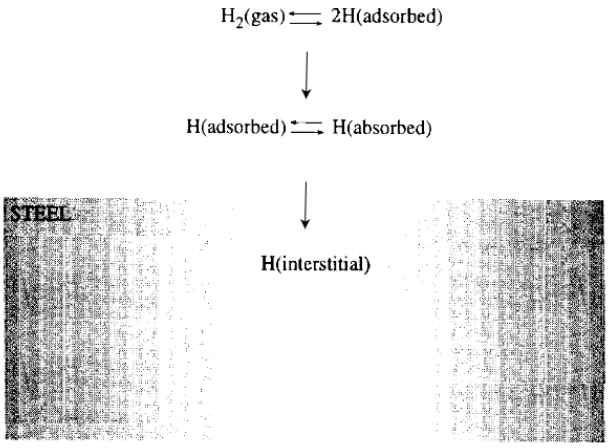

FIGURE 2.2: Illustration of the penetration of atomic hydrogen in carbon steel for a hydrogen environment [7].

The penetrated atomic hydrogen will diffuse into the crystal structures of the material. Atomic hydrogen has a low solubility and high diffusivity which makes the atoms sensitive to trapping [9]. Trapping is the diffusion of atomic hydrogen through the material at traps, which are spaces in the material that results from dislocations, grain boundaries, internal voids, cracks, particle-matrix interfaces and solute atoms [8].

The presence of atomic hydrogen in the crystal structures of the material can have a negative effect on the material strength and ductility of the pipeline [8]. A study conducted by DNV GL [10] shows that the transition from hydrocarbon transport to hydrogen transport in carbon steel pipelines will indeed change the material behaviour of the pipeline. However, these changes will not endanger the feasibility of hydrogen transport in onshore pipelines. This is positive for the feasibility of hydrogen transport in offshore pipelines, because onshore pipelines are made of the same carbon steel material as offshore pipelines. An overview of the material changes in the offshore pipeline is given in Appendix A.

The changes in material behaviour also include a change in fatigue behaviour [10]. In onshore pipelines and buried offshore pipelines, the only fatigue forces are from internal pressure cycles, this is because they are not subjected to environmental loads. The frequency of pressure cycles is relatively small. Therefore, it will not lead to high fatigue damage in the material. The fatigue forces can be several times bigger in exposed offshore pipelines compared to onshore pipelines or buried offshore pipelines. Therefore, the change in fatigue behaviour will have to be analysed extensively for the feasibility of hydrogen transport in offshore pipelines. The main source of fatigue in offshore pipelines is due to Vortex-induced vibrations in freespans. Vortex-induced vibrations are discussed extensively in the next section.

2.2 Vortex-induced vibrations

Sediment transport at the seabed could change the seabed topology around offshore pipelines, which can lead to the formation of freespans. Freespans are parts of a pipeline that are not supported by the seabed, as shown in Figure 2.3. The presence of near-seabed currents can lead to vibrations of these freespans, the so-called Vortex-induced vibrations (VIV). These vibrations can lead to fatigue damage in the material, and eventually to fatigue failure of the offshore pipeline.

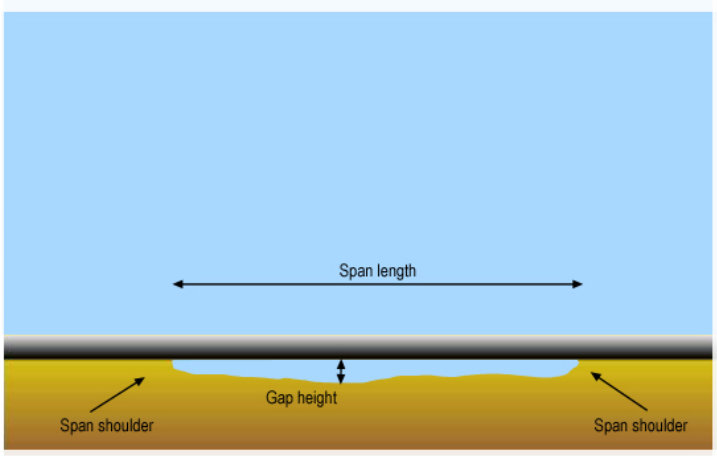

FIGURE 2.3: Offshore freespan. The span shoulders, span length and gap height are indicated.

2.2.1 Vortex shedding

If a near-seabed current is subjected to a pipeline, vortices can be formed in the wake of the cylinder, as shown in figure 2.4. These vortices detach periodically from the upper and lower side of the pipeline so that they create a vortex street in the wake of the cylinder.

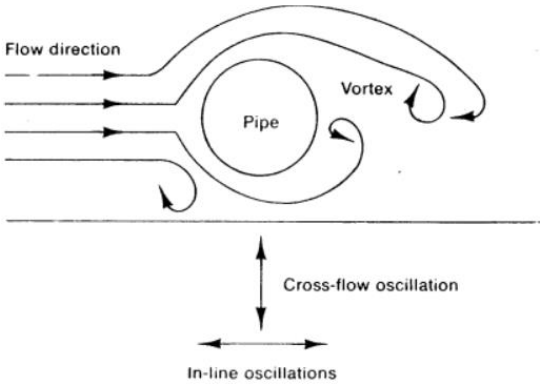

FIGURE 2.4: Vortex shedding [11]

The water particles of the current that is subjected to a freespan are forced to flow around the pipeline. The roughness of the outer pipeline surface creates a boundary layer that causes the water particles to move slower near the pipeline surface than the water particles further away from the outer pipeline surface. If the boundary layer has passed the top or bottom of the pipeline, it will separate from the surface of the pipeline and form a shear force flow. These flows results in low-pressure vortices in the wake of the pipeline [12]. The pipeline is attracted towards the low-pressure vortices. Therefore, the pipeline could start to vibrate.

The vibrations will be determined in the in-line direction (IL) and cross-flow direction (CF), as indicated in Figure 2.4.

The shape of the vortices in the wake of the pipeline is dependent on the Reynolds number, which can be determined using formula 2.1. Figure 2.5 displays an overview of the different vortex shedding regimes. Offshore pipelines have typically a Reynolds number in between 300 and $3 * 10^5$ [13], which results in a fully turbulent vortex street.

$$Reynolds\ number : Re = \frac{V\ D}{v} \tag{2.1}$$

V is the near-seabed current velocity $[\frac{m}{s}]$

D is the outer diameter of the pipeline $[m]$

v is the kinematic viscosity $[\frac{m^2}{s}]$

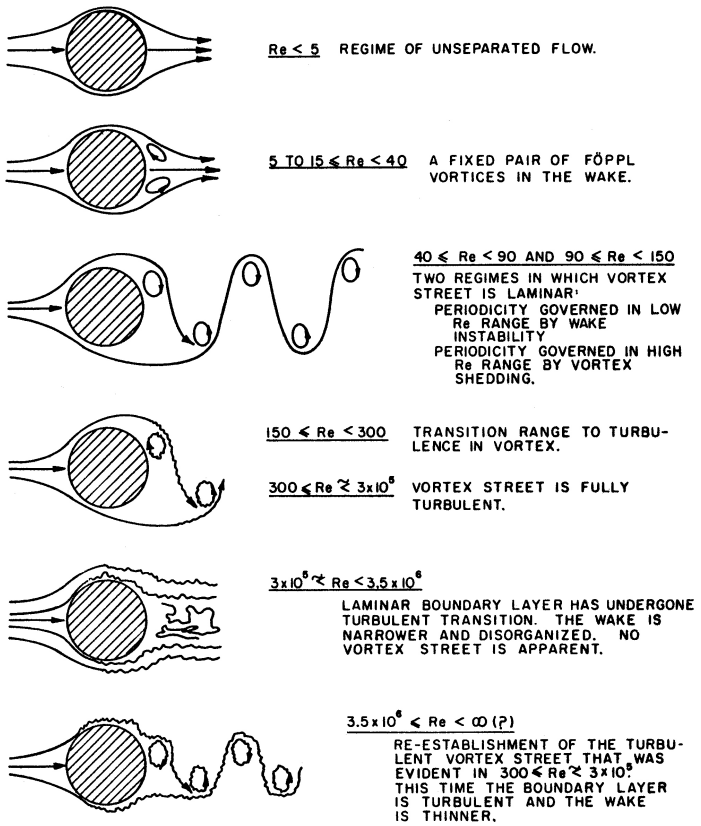

FIGURE 2.5: A overview of the vortex shedding regimes regimes for different Reynolds number regimes [13].

The shedding frequency is the frequency at which the vortices shed and is calculated using formula 2.2. This formula includes the Strouhal number St, which is an adimensional number to determine the oscillation of the vortices. For cylinders, the Strouhal number is 0.2 [13].

$$Shedding\ frequency : f_s = \frac{V\ St}{D} \tag{2.2}$$

St is the Strouhal number $[-]$

2.2.2 Lock-in region

When the vortex shedding frequency is equal to the natural frequency of the freespan, it is expected that the VIV have a maximum amplitude of vibration. The lock-in phenomena takes place if the shedding frequency becomes close to the natural frequency of the freespan. In this lock-in region, the shedding frequency will stick to the natural frequency of the freespan. An idealised depiction of the lock-in region for cross-flow direction is shown in figure 2.6. As shown in the figure, the lock-in region is dependent on the reduced velocity. The reduced velocity is a dimensionless value that can be determined with formula 2.3.

$$Reduced\ velocity : V_r = \frac{V}{f_n\, D} \tag{2.3}$$

f_n is the natural frequency of the freespan $[\frac{1}{s}]$

The maximum amplitude is expected when the natural frequency is equal to the shedding frequency. Equalising these two frequencies and then subsidising the shedding frequency in the reduced velocity formula shows that the maximum amplitude of vibrations is expected at a reduced velocity of 1 divided by the Strouhal number. Therefore, the maximum VIV amplitude for freespans is expected at a reduced velocity of 5.

The freespan length influences the natural frequency of a freespan. If the freespan length increases, the natural frequency of the freespan will decrease. Therefore, the reduced velocity increases and the pipeline will vibrate at lower near-seabed velocities.

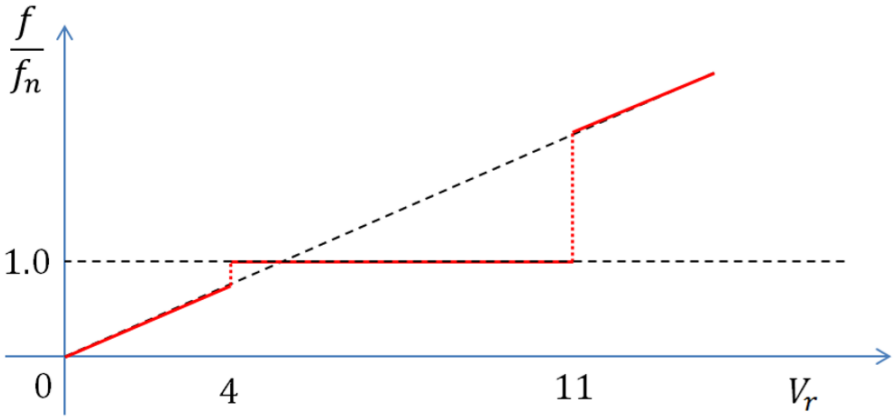

FIGURE 2.6: Lock-in region [6]

2.2.3 Bending stress

Internal stress in the pipeline's material will occur if there are VIV in a freespan. The total stress in the material is a summation of the normal stress and shear stress. Only the normal stress has a significant influence on the fatigue behaviour in offshore pipelines [14]. Therefore, only the normal stress will be evaluated in this research.

The normal stress is dependent on the bending moment and the axial force in the cross-section of the pipeline. As shown in figure 2.7, the bending moment increases with the radius from the centre of the pipeline. Therefore, the normal stress has a maximum value at the outer surface of the pipeline. The normal stress is also varying over the length of the freespan.

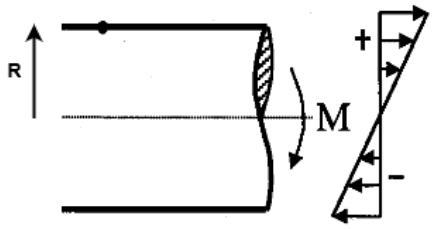

FIGURE 2.7: Bending moment over the cross-section of the pipeline. [15]

2.3 Fatigue behaviour

Fatigue is a phenomenon in which material can fail due to fluctuating stresses at a lower stresses level than the yield stress. The fluctuating stresses result in dislocation tangles which harden the material, from which a crack could arise. This crack could grow to a critical size due to the persistent stress cycles [16]. The total fatigue damage in a material depends on the total number of stress cycles that material has experienced and the stress ranges of these stress cycles.

As described in section 2.2, stress oscillations due to VIV could eventually lead to fatigue failure in offshore pipelines. Although the fatigue behaviour in materials has extensively been investigated, it is not possible to predict the exact number of stress cycles that will lead to fatigue failure. This section discusses the theory of fatigue behaviour that is needed to analyse the fatigue behaviour of the specified pipeline.

2.3.1 SN-curve

A fatigue curve, or SN-curve, is a material specific plot that can determine the expected fatigue limit for a given stress range. The fatigue limit is the maximum amount of stress cycles that lead to fatigue failure in the material for a given stress range. The fatigue damage is expressed in the percentage of the fatigue limit. SN-curves are used to calculate the expected fatigue damage in a material. Figure 2.8 shows an example of a SN-curve. It can be seen in this figure that a higher stress range results in a lower number of cycles to fatigue failure.

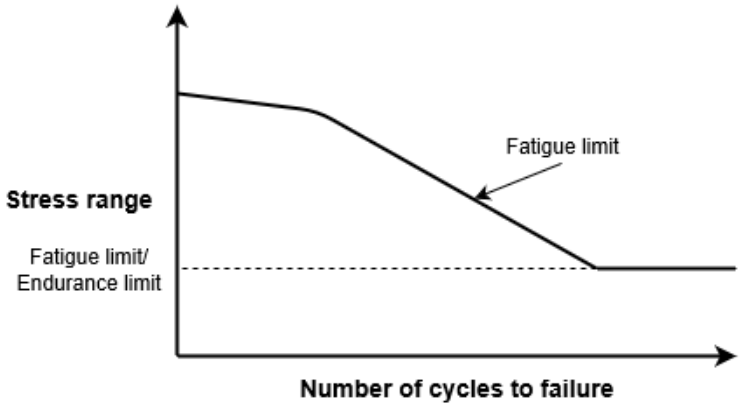

FIGURE 2.8: Example of a SN-curve for a material (plotted on log-log axes)

2.3.2 Fatigue phases

Three phases of fatigue behaviour can be distinguished: crack initiation, crack growth and failure. If most of the fatigue life consists of the fatigue crack initiation phase, then it is called initiation-controlled fatigue, and if the largest part of the fatigue life consists of fatigue crack growth, it is called propagation controlled fatigue [16]. The different phases are discussed in the following subsections.

Fatigue crack initiation

The varying stress hardens the material. This can lead to dislocation tangles, from which a crack can arises. Crack initiation usually occurs at the surface of a material [17]. The dimensions of which a dislocation becomes a crack are not given in any standards. Therefore, most engineers speak of a crack when the crack detection equipment is able to detect it [18].

Fatigue crack growth

The fatigue crack growth begins after a crack has occurred in the material. The rate at which a crack grows per stress cycle depends on the material and the cyclic stress intensity range ΔK [Pa $\sqrt{m}$].*The*ΔK is dependent on the stress range and the length of the crack, as shown in formula 2.4. The length of the crack will increase over time. Therefore, ΔK will also increase. Figure 2.9 schematically displays the relationship between the crack growth rate per cycle versus ΔK. This relation is called Paris' law. It can be seen from figure 2.9 that cracks will not grow if the cyclic stress intensity factor is below the ΔK threshold value.

$$Cyclic\ stress\ intensity\ range : \Delta K = \Delta\omega\sqrt{\pi c} \tag{2.4}$$

$\Delta\omega$ is the stress range [Pa]
c is the crack length[m]

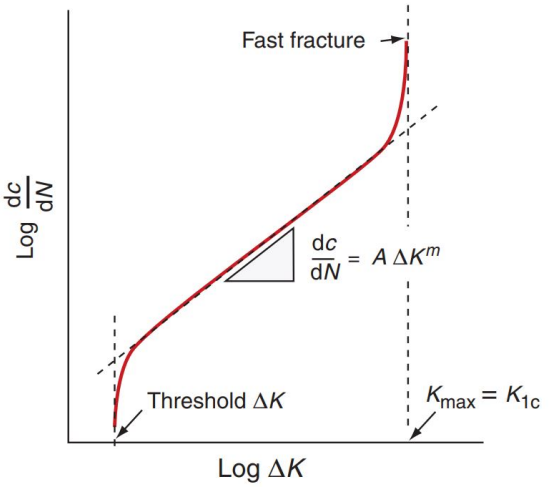

FIGURE 2.9: Paris' law [16]

The crack growth velocity describes the growth velocity of a crack during cycling loading. This velocity is dependent on the fatigue crack growth rate and the stress cycle frequency.

The crack will be stretched during each stress cycle. Due to this, a plastic zone will occur at the crack tip, as indicated in figure 2.10. In this zone the material is stretched and a new surface of the crack occurs, as shown in the figure. This leads to crack growth in the direction of r, as indicated in figure 2.10.

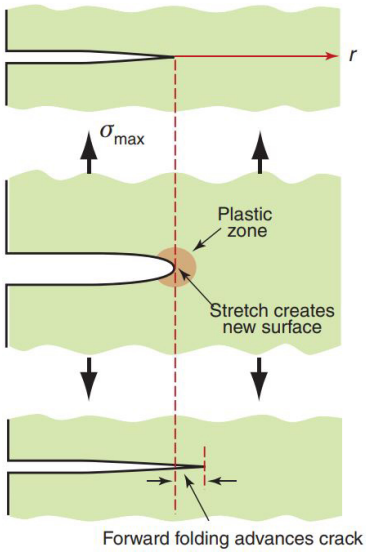

FIGURE 2.10: The cyclic loading forms a plastic zone at the crack tip [16]

.

Fatigue failure

During the fatigue crack growth phase, the ΔK grows until it reaches its maximum value. At this maximum value, the material fails during a single cycle, as shown in Figure 2.9. This maximum value is called the fracture toughness K_{Ic} [16].

2.4 Change in fatigue behaviour due to atomic hydrogen

As discussed in section 2.1, the presence of atomic hydrogen in the material will influence the fatigue behaviour of carbon steel material. It is not known in open literature what the influences are of the presence of hydrogen on the crack initiation phase. The influence of hydrogen on the crack growth phase is described in the literature.

The cycling loading creates a hydrostatic tension at the crack tip. This hydrostatic tension creates spaces between the atomic layers, which will attract the atomic hydrogen that is penetrated in the material. Therefore, the atomic hydrogen in the pipeline's material will diffuse to the plastic zone of a crack tip, as shown in figure 2.11. The cohesion theory explains the increase in fatigue crack growth due to the presence of the atomic hydrogen in the crack tip [19]. This theory states that the high concentration of hydrogen atoms in the plastic zone leads to a local reduction in the binding forces between atomic layers. This reduces the local critical tensile tension, which increases crack growth.

The influence of atomic hydrogen in a material on the crack growth rate is dependent on the crack growth velocity. If the crack growth velocity is low, the hydrogen atoms have enough time after a stress cycle to diffuse to the displaced crack tip. This causes the hydrogen atoms to

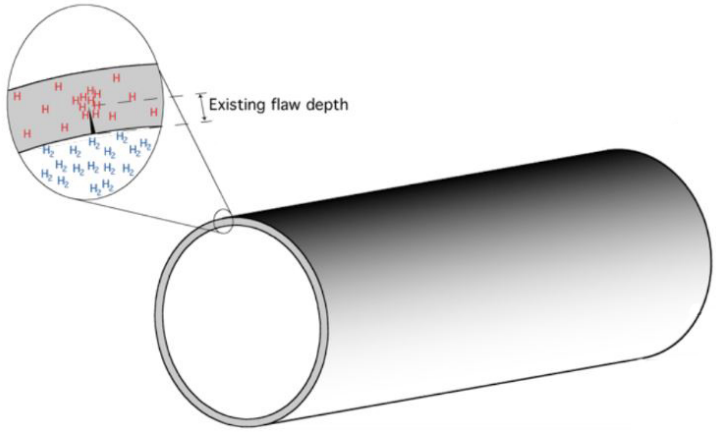

FIGURE 2.11: Atomic hydrogen will diffuse to the plastic zone of the crack tip. Atomic hydrogen in indicated with single red H and hydrogen molecules are indicated with blue H_2 [20]

.

influence the crack growth rate of the next stress cycle. This is called the saturated condition [21]. If the crack growth velocity is above a specific value, the crack growth velocity is higher than the diffusion velocity of the atomic hydrogen to the displaced crack tip [19]. Therefore, the atomic hydrogen concentration in the displaced crack tip will be lower. This results in less influence of the atomic hydrogen on fatigue crack growth rate. Therefore, the fatigue crack growth rate will be lower. This is called the non-saturated condition [21].

The fatigue crack growth caused by VIV for hydrogen transport in offshore pipelines will be in the saturated condition. Therefore, fatigue testing in a hydrogen environment needs to be done with a low-stress cycle frequency. Low-frequency fatigue crack growth tests for different types of carbon steel materials are carried out by TWI [22], TNO [23] and Sandia National Institute [20]. The test results of Sandia National Institute are shown in Figure 2.12. The fatigue tests for hydrogen environment are performed with a saturated frequency, and the fatigue tests in the air are performed at a rate of 10 Hz. The figure confirms that the fatigue crack growth rate for a pipeline that transport hydrogen can be higher than for a pipeline filled with air. A wide variety of pipeline steels display nominally the same fatigue response in high-pressure gaseous hydrogen of 210 bar.

The fatigue crack growth tests carried out by TWI, TNO and Sandia National Institute are conducted in an in-situ hydrogen environment. In-situ hydrogen charging is needed because the atomic hydrogen will diffuse out of the test material if this hydrogen containing test material is placed in air.

Due to the change in fatigue crack growth between both environments, it is known that the SN-curves for carbon steel material will change due to the presence of atomic hydrogen in the material. The SN-curve for carbon steel materials in a hydrogen environment is not known in the open literature [5]. Therefore, it is important to investigate the change in fatigue behaviour in a hydrogen environment before the fatigue behaviour of the specified pipeline can be assessed.

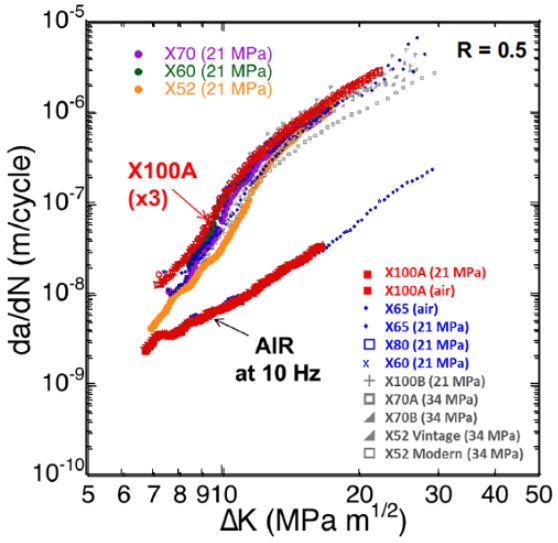

FIGURE 2.12: Fatigue crack growth test results for several types of carbon steel material. The tests have been carried out in both an air and an environment of hydrogen [20].

2.5 Conclusion

From experience in the oil and gas industry with the presence of hydrogen sulphide in carbon steel pipelines, it is known that atomic hydrogen in the material can lead to changes in material behaviour and degrades steel performance. The transport of hydrogen through the pipeline will also lead to the penetration of atomic hydrogen in the pipeline's material. The hydrogen concentration in the material that can occur with the presence of hydrogen sulphide in the pipeline is significantly higher than for the presence of hydrogen gas in the pipeline. It has been shown that for hydrogen transport, the atomic hydrogen will significantly degrade the steel performance. However, only the change in fatigue behaviour could endanger the feasibility of hydrogen transport through carbon steel pipelines. Therefore, this study will mainly focus on the fatigue behaviour in offshore pipelines.

VIV is a complex phenomena, yet well understood in literature. The bending of the pipeline due to VIV will result in stresses in the pipeline. It is discussed that only normal stress is relevant for the fatigue behaviour in the pipeline.

Fatigue crack growth data for carbon steel materials in a hydrogen environment is available in the open literature. This data shows that atomic hydrogen in the material could have a significant influence on the fatigue crack growth of carbon steel material. Unfortunately, there is less information available for the fatigue crack initiation phases and there is no SN-curve for carbon steel materials available in open literature.

SN-curves are used to calculate the expected fatigue damage in a material. Therefore, it is essential to approach the SN-curve for hydrogen environment before a fatigue assessment for a pipeline that transports hydrogen can be performed. The following chapter focuses on approaching the SN-curve in a hydrogen environment.

Chapter 3

Approach of the SN-curve in hydrogen environment

As discussed in section 2.3.1, SN-curves are used to calculate the fatigue damage of a pipeline based on the stress range of the stress cycles in the pipeline. The SN-curves from DNV-RP-C203 [24] are widely used in industry for fatigue calculations of pipelines. Those are material specific and constructed by doing laboratory fatigue tests. The SN-curve will change due to the presence of atomic hydrogen in the material of the pipeline. The SN-curve for the carbon steel material in hydrogen environment is not known in the open literature. Because laboratory fatigue tests in hydrogen environment are too expensive for this research, a model is derived that could predict the SN-curve in hydrogen environment.

To approach the SN-curve in a hydrogen environment, the comparison is made between the fatigue behaviour of materials in a hydrogen environment and the fatigue behaviour of materials in sour environments, of which more fatigue data is available. This comparison is made because in both environments atomic hydrogen will penetrate the pipeline's material and influences the fatigue behaviour. The difference with hydrogen sulphide is that the presence of atomic sulphide on the inner surface of the pipeline. The atomic sulphide will delay the recombination rate of free atomic hydrogen on the surface of the material. Therefore, the penetration rate of hydrogen atoms in sour environments is higher [8]. However, if the influence of the environment on the fatigue crack growth rate (FCGR) in a hydrogen environment are similar as for a specific sour environment, it is assumed that the amount of hydrogen atoms in the material is equal for both environments, and that it will result in similar change in fatigue in comparison with the fatigue behaviour in air.

Section 3.1 will discusses the method to approach the SN-curve for a material in a hydrogen environment with limited laboratory fatigue test data and discuss the assumptions that are made. After that, the SN curve for the specified pipeline is determined in section 3.2 based on available fatigue test data.

3.1 Method to approach an SN-curve in hydrogen environment

The method to approach the SN-curve for a material in a hydrogen environment is described in seven steps and can be applied to different materials in a hydrogen environments.

1. Compare the available fatigue crack growth data for hydrogen environment with fatigue crack growth data for sour environments. Find the sour environments that have similar conditions like that of a hydrogen environment and determine the knock down factors (KDF), or fatigue life reduction factor, for fatigue crack growth in both environments.

- The sour environment fatigue crack growth data is chosen from the Region 3 of the ISO 15156 Domain Diagram with observed saturated knock down factors (KDF_{ESat}).
- It is essential that the available fatigue crack growth data for both environments that are used for the comparison of the two environments must be obtained by tests that have similar test specifications.

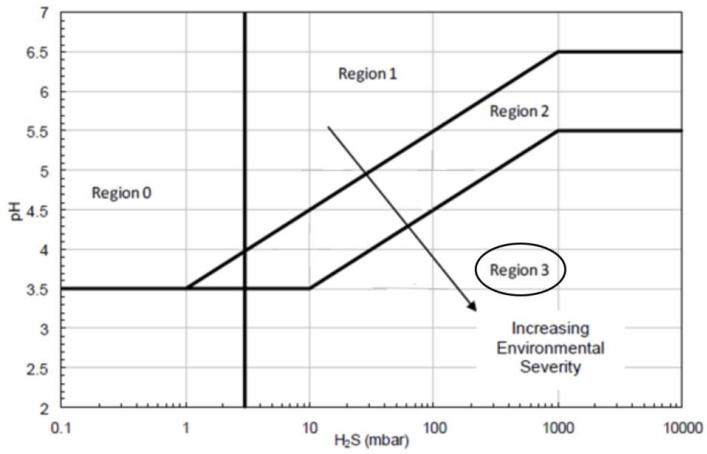

FIGURE 3.1: ISO 15156 Domain Diagram [21]

2. A penalty factor is introduced to account for the difference between the KDF for fatigue crack growth of a hydrogen environment and the average KDF for fatigue crack growth of the sour environment considered from region 3 of the ISO 15156 Domain Diagram with observed KDF_{ESat}. The penalty factor is calculated with formula 3.1.

$$Penalty\ factor = \frac{KDF_{hydrogen}}{KDF_{sour}} \tag{3.1}$$

$KDF_{hydrogen}$ is the knockdown factor for fatigue crack growth in hydrogen environment $[-]$
KDF_{sour} is the knockdown factor for fatigue crack growth in sour environment $[-]$

- A minimum penalty factor of 1 is used.

3. Calculate the saturated KDF for the SN-curve for environments in Region 3 of the 15156 Domain Diagram [21].
   - The KDF_{ESat} relates data where the saturated condition is reached. This value is most conservative.
4. Approach the saturated SN-curve data for the sour environment that corresponds with the saturated frequency, with formula 3.6 [21].

$$N_{crit} = \frac{10^{x}}{KDF_{ESat}} \cdot (\Delta\sigma)^{-n} \tag{3.2}$$

KDF_{ESat} is the saturated KDF for SN-curve $[-]$
$\Delta\sigma$ is the stress range $[Pa]$

- The SN-curve data is material specific. The parameters x and n scale the SN curve data to the type of the material that is being examined. These can be found in DNV-RP-C203 [24].

5. Multiply the saturated SN-curve data with the penalty factor to approach the saturated SN-curve in a hydrogen environment.
6. To find the SN-curve data for higher frequencies than the saturated frequency, the saturated SN-curves data need to be multiplied with L(f), as shown below [21].

$$N = N_{crit} \cdot L(f) \tag{3.3}$$

N_{crit} is the numbers of stress cycles to failure for the saturated condition $[-]$

$$L(f) = 1, for f < f_{crit} \tag{3.4}$$

$$L(f) = (\frac{f}{f_{crit}})^{m1}, for f > f_{crit} \tag{3.5}$$

m_1 is the slope between frequency and the obeserved KDF for SN-curve $[-]$
f_{crit} is the critical (or saturated) frequency $[Hz]$

- At frequencies above the saturated frequency, the saturated condition will not be reached, and fatigue lives will be longer. This is because the fatigue crack growth at frequencies higher than the saturated frequency will be faster than the diffusion of hydrogen atoms to the crack tip.
- The critical frequency is depended on the stress range. At low stress ranges the critical frequency is higher, so the influence of the frequency is less noticeable.

7. Plot the SN-curves in a graph together with the SN-curve for the material in air.

3.2 SN-curve for carbon steel in hydrogen environment

The method that is derived in section 3.1 to approach the SN-curve for material in a hydrogen environment is used in this section to derive the SN-curve for the carbons steel pipeline.

1. Compare the available fatigue crack growth data for hydrogen environment with fatigue crack growth data from sour environments. Find the sour environments that have similar conditions like that of a hydrogen environment and determine the knock down factors (KDF), or fatigue life reduction factor, for fatigue crack growth in both environments.
    - The test specimens of the fatigue crack growth tests of Sandia National Institute are fully exposed to high pressure hydrogen gas using fracture mechanics specimens such as CT or ESET specimens. The test specifications of the sour environment tests, obtained from Safebuck 3 [21], are similar to those of the hydrogen environment tests of Sandia National Institute. For fatigue crack growth data in hydrogen environment, only results are available for fully exposed specimens. Therefore, the comparison is made between results with fully exposed specimens.
    - From test data of Sandia National Institute we can deduct that for fatigue crack growth in pure hydrogen, the saturated frequency is around 0.1 Hz, and the saturated KDF is 60. (2x KDF (1 Hz))
2. Calculate the penalty factor that shows the difference between the KDF for fatigue crack growth of a hydrogen environment and the average KDF for fatigue crack growth of the sour environment considered from region 3 of the ISO 15156 Domain Diagram.
    - The penalty factor is calculated with formula 3.1.
3. Calculate the saturated KDF for the SN-curve for environments in Region 3 of the 15156 Domain Diagram.
4. Approach the saturated SN-curve data for the sour environment that corresponds with the saturated frequency.
    - The design values x=11.855 and n=-3 are associated with the standard class F curve from DNVGL-C203. Standard class F curve is used in industry to assess the girth welds of carbon steel pipelines in air.

$$N_{crit} = \frac{10^{11.855}}{KDF_{sat}} \cdot (\Delta\sigma)^{-3} \tag{3.6}$$

5. Multiply the saturated SN-curve data with the penalty factor to approximate the saturated SN-curve in a hydrogen environment.
6. To find the SN-curve data for higher frequencies than the saturated frequency, the saturated SN-curves data need to be multiplied with L(f), as shown below.
    - Based on information from Sandia National Institute, a saturated frequency of 0.1 Hz is used. The stress range due to Vortex-induced vibrations that are of interest in freespan analysis will be small. Therefore, we assume the saturated KDF for the SN-curve for VIV frequencies of 0.5 - 2 Hz.
7. Plot the SN-curves in a graph together with the SN-curve for the material in air.

3.3 Conclusion

The method to approach an SN-curve in hydrogen environment with limited available fatigue data is explained in section 3.1. It shows that a large number of assumptions is needed to make the comparison between hydrogen gas and sour environments.

The derived SN-curve for carbon steel in hydrogen environment shows that the influence of hydrogen on the fatigue behaviour of carbon steel is significant. Therefore, it is important that the fatigue behaviour in the specified pipeline will be further investigated. The SN-curve for carbon steel material in hydrogen environment is used in the fatigue analysis of specified pipeline that is described in the next chapter.

3.4 Discussion on the method

For the approach of the SN-curve of material in hydrogen environment, it is assumed that the crack initiation phase in a hydrogen environment is similar to that in a sour environment when the fatigue crack growth phase is similar. This assumption is questioned by recently published papers [25, 26]. Based on these papers, it would appear that the fatigue crack growth phase that is tested with pre-existing crack specimens is similar for both environments, but that the initiation phase in a nominally perfect material is different. It would appear that hydrogen has less effect on the initiation.

Fatigue crack growth is dependent on the pressure of the environment [5]. In sour environments, higher partial pressure or hydrogen sulphide leads to a higher KDF's [21]. Therefore, it is expected that that higher pressures in a hydrogen environment lead to higher KDF's. The fatigue crack growth tests of Sandia National Institute are conducted for a hydrogen pressure of 210 bar, and the operational pressure in the specified pipeline has a maximum of 110 bar. Therefore, the use of the Sandia National Institute data gives conservative results concerning pressure.

Chapter 4

Fatigue analysis for specified pipeline

4.1 Introduction

This chapter discusses the fatigue analysis of the specified pipeline that assess the change in fatigue behaviour due to the transition from hydrocarbon transport to hydrogen transport. This analysis considers hydrogen transport through the specified pipeline for the next 32 years. A term of 32 years has been chosen because it is only lucrative to make the transition to hydrogen if it is feasible for at least 30 years.

The fatigue damage calculations are performed with the freespan modelling program Fatfree. Fatfree is an Excel spreadsheet developed by DNV GL for the assessment of freespans in offshore pipelines. It allows the user to model the pipeline with a large set of input parameters and to implement site-specific metocean data.

The pipeline is made from carbon steel X60 material and has no internal coating.

4.2 Pipeline sectioning

The pipeline is divided in sections. Each section has a unique set of parameters that is an input for fatigue calculation of observed freespans within the section. These parameters are the concrete thickness, the bearing and the metocean data; wave and current data, soil specifications and water depth.

4.3 Site-specific wave and current data

The site-specific wave and current data are used [27]. Long-term probability distributions for current and waves are given as directional data with a given probability. In this analysis, the current is modelled in U_c histograms, and the waves are modelled in H_s-T_s scatter diagrams.

4.4 Historical freespan data

To determine the existing fatigue damage of the selected pipeline, the fatigue history of the pipeline must be considered. Through sonar surveys, it is known when and where freespans have occurred. They show that there are significant changes in freespans per year.

The existence times of the detected freespans are calculated as the time between the last inspection before the freespan was identified at a specific kilometres point (KP) and the first inspection after the freespan had disappeared at the same KP, divided by two.

4.5 Assumptions for the fatigue analysis

To perform the fatigue analysis for both cases, the following assumptions have been made:

- Freespans before 2000 and after 2017 will be at the same KP's like the freespans between 2000 and 2017.
- Freespans before 2000 and after 2017 will have the same average existence time per year as the freespans between 2000 and 2017.
- The limit pressure of the specified pipeline, 110 bar, has been used as the operating pressure for hydrogen transport.

4.6 Partial safety factors

The important span characteristics, like span length and the span gap, are measured with a high degree of accuracy, and the metocean data and soil conditions are also well known. Therefore, the "Very well defined" safety factor class is used in the fatigue analysis. This safety factor class contains the lowest partial safety factors that can be used in the DNV Free Spanning Assessment Methodology [28], which are displayed in 4.1.

Partial safety factor	Value	Applies to
η	0.50	Fatigue life
γ_k	1.15	Total damping
$\gamma_{f,IL}$	1.00	IL natural frequency
$\gamma_{f,CF}$	1.00	CF natural frequency
γ_s	1.30	Stress ranges
$\gamma_{on,IL}$	1.10	IL VIV-onset
$\gamma_{on,CF}$	1.20	CF VIV-onset

TABLE 4.1: Partial safety factors for the fatigue damage calculations

The partial safety factor η is used over the determined fatigue life. Therefore, it is possible to not take this partial safety factor into account by multiplying the final fatigue life by a factor of 2.

4.7 Method

This fatigue analysis for the specified pipeline makes the comparison between two cases: a hydrogen case that includes a transition from hydrocarbons transport to hydrogen transport in 2020, as shown in figure 4.1, and the hydrocarbons case in which the pipeline transports hydrocarbons for the entire existence time of the pipeline, as shown in figure 4.2. These timelines show that the fatigue analysis begins in 1990, the year when the pipeline is installed on the seabed and ends in 2052, 32 years after the transition year 2020.

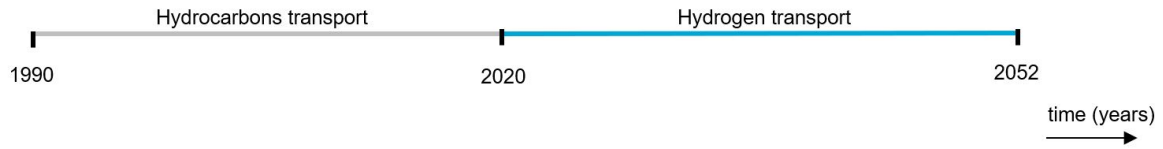

FIGURE 4.1: Timeline for the hydrogen case

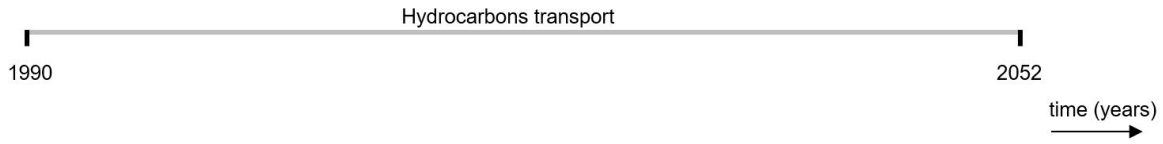

FIGURE 4.2: Timeline for the hydrocarbon case

The fatigue analysis consists of the following four steps and is conducted for both the hydrogen transport case and the hydrocarbons case:

1 Calculate the cumulative existence time of each freespan. This calculation is based on the historical freespan data and the assumptions from section 4.5.

2 Calculate the fatigue damage per year in each freespan with Fatfree.

3 Calculate the accumulated fatigue damage in 2052 in each freespan.

4 Determine which freespans do not fit the acceptance criteria of DNV-RP-F105. The acceptance criteria is 10 percent of the fatigue limit.

4.8 SN-curves

A set of two SN-curves is used to determine the fatigue damage in the pipeline. One for the fatigue damage calculations at the inner surface of the pipeline and one for the fatigue calculations at the outer surface of the pipeline. In the hydrocarbon case, the two SN-curves are different due to cathodic protection at the outer surface of the pipeline. Cathodic protection protects the pipeline's material against corrosion by the sea water but has a negative effect on the SN-curve. The SN-curves for pipelines with and without cathodic protection are from DNV-RP-C203 [24]. In the hydrogen case, the SN-curve for the inner surface is different due to the presence of hydrogen in the pipeline. The SN-curve for the pipeline material in hydrogen environment has been derived in chapter 3. The fatigue damage calculation that results in the highest fatigue damage between the inner and outer wall surface is leading.

4.9 Fatigue analysis results

In this section, the results of the fatigue analysis with Fatfree is discussed. First, the fatigue damage per year is shown for each freespan in both the hydrogen case and the hydrocarbon case. After that, the accumulating fatigue for both cases is determined for 2052. The expected accumulated fatigue is calculated with the fatigue damage rate per year and the estimated number of existence years of the freespans. The acceptance criteria for fatigue damage in offshore freespans is a maximum of 10 percent of the fatigue limit, based on DNV-RP-F105 [28].

4.9.1 Fatigue damage per year

The transition from hydrocarbons transport to hydrogen transport leads to an increase in the expected fatigue damage rate. This increase in fatigue damage rate, in turn, leads to an increased probability of fatigue failure of the pipeline due to VIV. The existence time will need to be reduced to decrease this increased probability of fatigue failure. This is possible by increasing the survey frequency and by applying earlier mitigations.

The results of fatigue damage per year also show that higher freespan lengths lead to higher expected fatigue damages per year. This can be explained by the frequencies and the lock-in region, as discussed in section 2.2. The natural frequency of a freespan will decrease if the freespan length becomes longer, which results in a higher reduced velocity. This will increase the chance that the reduced velocity is in the lock-in region, which means that there is a higher chance that the pipeline will vibrate with a relatively high amplitude. Therefore, larger freespans will have higher expected fatigue damage per year.

4.9.2 Accumulated fatigue damage

The accumulated fatigue damage is a multiplication of the fatigue damage per year and the estimated existence time of the pipeline in years. The estimated number of existence years are determined based on the assumptions of section 4.5. The accumulated fatigue damage results in 2052 show which freespans do not fit the acceptance criteria.

In the hydrogen case, the amount of critical freespans is 50 percent higher compared to the hydrocarbons case. Therefore, the transition from hydrocarbons transport to hydrogen transport will lead to an increase in number of freespans at which mitigation potentially needs to be applied. This will increase the expected mitigation costs for the pipeline.

4.10 Conclusion

The purpose of this chapter was to assess the change in fatigue damage rate in all the freespans due to the transition from hydrocarbon transport to hydrogen transport and to assess the feasibility of hydrogen transport through the specified pipeline for the next 32 years.

It is not possible to predict the exact locations of future freespans. Therefore, future freespans are assumed in section 4.5 to occur at exactly the same locations as the freespans detected between 2000 and 2017. The accumulated fatigue damage rate at each location between 1990 and 2052 is, therefore, a summation of the fatigue damage rates of all the freespans that have occurred at a specific location.

Section 4.9 shows that the transition to hydrogen transport leads to an increase in fatigue damage rate for all the freespans of the pipeline. This increase is mainly due to the new SN-curve for hydrogen environment. The decrease of content density and the increase in operational pressure for the hydrogen case do not have a significant influence on the fatigue damage rate.

The transition to hydrogen transport through the pipeline will increase the number of freespans that do not fit the acceptance criteria of a maximum accumulated fatigue damage rate of 10 percent of the fatigue limit. If a lifetime till 2052 is considered, this number will increase by 50 percent. This increase results in higher expected mitigation costs of the pipeline.

The main concern of the fatigue analysis results is the increased fatigue damage rate of the critical freespans, because the probability of fatigue failure in the freespans becomes higher. To avoid this increase, the allowable existence time of these freespans needs to be reduced. If no adjustments will be made, safe transport of hydrogen through the pipeline cannot be ensured for the next 32 years. Therefore, the increased probability of fatigue failure in the critical freespan endangers the feasibility of hydrogen transport through the specified pipeline.

The following chapter discusses the adjustments that can be made to reduce the increased probability of fatigue failure in critical freespans.

Chapter 5

Adjustments to the specified pipeline

5.1 Introduction

It was shown in chapter 4 that the transition from hydrocarbon transport to hydrogen transport increases the probability of fatigue failure in freespans. The probability of fatigue failure is too high to ensure hydrogen transport in a safe way. This chapter discusses the adjustments that can be made to avoid the increase in probability of fatigue failure.

Two adjustments are considered. Firstly, an increase of the survey frequency to decrease the possible existence time of freespans. Secondly, preventing the formation of freespans by applying preventive mitigation. A comparison between the costs of both options results in a preferred option.

5.2 Increase of the pipeline surveys

If the survey frequency is increased, critical freespans could be detected and mitigated in an earlier phase. An increased survey frequency will not reduce the fatigue damage rate in the pipeline, but it will decrease the probability of fatigue failure of the pipeline. This is because the possible existence time of critical freespans between the surveys decreases.

The ratio between the fatigue damage rates for hydrogen case and the hydrocarbon case is around 15 for the freespans of interest. Therefore, the survey frequency needs to be increased with a factor 15 to decrease the probability of fatigue failure by this factor. For hydrocarbon transport, the surveys are conducted every two years. If a multiplication factor of 15 is applied for hydrogen transport, a survey will have to be carried out every 48 days.

5.2.1 Pipeline survey costs

When a critical freespan is detected during a survey, it will need to be mitigated. Therefore, in addition to the survey costs, there are also mitigation costs that need to be added to the survey cost.

5.3 Preventive mitigation

Freespans occur due to a substantial migration of the soil under the pipeline. To significantly reduce the likelihood of the formation of critical freespans, we can apply preventive mitigation that will avoid the migration of the soil under the pipeline. This section discusses two

types of preventive mitigation, namely to bury parts of the pipeline at a certain depth or to apply rock dumping on parts of the pipeline. An additional advantage of these preventive mitigations is that it minimises the risk of third party damages.

5.3.1 Rock dumping on the pipeline

Rock dumping is a common way of freespan mitigation. The rocks are poured into the freespan to support the pipeline and thus reduce or eliminate the freespan. Rocks can also be deposited onto the pipeline to prevent seabed migration. This preventive mitigation will result in no freespans at these locations.

Rock dumping can lead to scouring at the ends of rock dumping. This can be prevented by installing anti-scour frond mattresses at these ends.

5.3.2 Trenching of the pipeline

The pipeline is installed on the seabed. It is possible to bury the pipeline to avoid the formation of critical freespans. This can be done with post-lay trenching that removes the seabed under the pipeline to lower the pipeline.

5.3.3 Critical pipeline sections

To avoid the formation of critical freespans in the pipeline, it is essential to understand how freespans are created and in which sections of the pipeline it is likely that freespans will occur. To this end, a seabed migration analysis has been performed as described in appendix B. This analysis was carried out with historical freespan data and seabed migration data. The result is displayed in table B.1. All the pipeline sections have received a rate between 1 and 3 for the 'freespan occurred between 2000-2017', in which 1 means that no freespans are observed between 2000 and 2017, 2 means that a small amount of freespans has occurred in this section, and 3 means that several freespans have detected in this sections. Also, all the pipeline sections have received a rate between 1 and 3 for the 'Sand wave migration level', in which 1 means that there is a low amount of sand wave migration activity, 2 means that there is a medium amount of sand wave migration activity and 3 means that there is a large amount of sand wave migration activity. These probability values are composed of the two rates and give the likelihood that future freespans will occur in these pipeline sections.

Section	**Freespans detected 2000-2017(1-3)**	**Seabed migration level(1-3)**	**probability(1-3)**
A	2	1	2
B	1	1	1
C	1	1	1
D	3	3	3
E	1	3	2
F	1	3	2
G	3	3	3
H	1	2	1
I	1	3	2
J	1	1	1
K	1	1	1

TABLE 5.1: probability analysis for freespans in the different sections of the pipeline.

Pipeline sections D and G have probability level 3 which means that these sections are susceptible to the formation of freespans. Therefore, preventive mitigation is considered for these pipeline sections.

5.3.4 Costs for preventive mitigation

The cost of preventive mitigation methods depends on fixed costs and variable costs. The fixed costs exist of mobilisation and demobilisation costs, project management costs and engineering costs. The variable costs are the operational and material costs, which mainly comprise the cost of renting a ship.

5.4 Results

The consideration of the most attractive adjustment is based on the cost. Rock dumping is the cheapest option. Therefore, rock dumping on the critical sections of the pipeline is recommended to ensure the safety of hydrogen transport in the specified pipeline.

5.5 Conclusion

Increasing the survey frequency by a factor of 15 as well as preventive mitigation by means of pipeline trenching or rock dumping are adjustments that will avoid the increased probability of failure in freespans due to the transition to hydrogen transport. A probability analysis for the formation of future freespans in different pipeline sections in appendix B, shows that only two sections pose a high probability to forming critical freespans. These sections must be mitigated to avoid the increased probability of fatigue failure.

Since all three mitigation options can avoid the increased probability of failure of the pipeline, the adjustments are compared by costs. Financial analysis shows that preventive mitigation by rock dumping of the critical pipeline sections has the lowest cost. Therefore, this preventive adjustment is the recommended option.

Chapter 6

Time-domain numerical model for freespans

6.1 Introduction

The DNV GL freespan modelling program Fatfree, based on DNV Free Spanning Methodology [28], is widely used in the offshore industry although the industry sees DNV Free Spanning Methodology as a very conservative approach. In this research, an existing time-domain numerical model is extended in order to study the fatigue behaviour of the pipeline subject due to VIV. The first sections of this chapter describes the parts that existing the model to be able to determine the stresses and fatigue behaviour in the pipeline. An overview of the additional components is shown in figure 6.1. Section 6.5 presents the comparison between Fatfree and the time-domain numerical model for freespans. This comparison shows the difference in the results between both programs.

The existing time-domain numerical model is developed for the thesis "Dynamic Interaction of Subsea Pipeline Spans due to Vortex-induced Vibrations" of Slingsby [6]. The model is programmed in the numerical computing program MATLAB. The model can simulate VIV due to uniform stationary flows in freespans of subsea pipelines. The vortices are modelled by a semi-empirical model called a wake oscillator. The pipeline is modelled as an Euler-Bernoulli beam using the finite element method. In contrast with industry used freespan analysis programs like Fatfree, the model can estimate the dynamic behaviour of a pipeline in time-domain. Therefore, it could includes non-linear calculations and determine the deflection of the pipeline over the entire length of the freespan. A force model is used that couples the equations of motions to the forces on the pipeline. A modal analysis is used to determine the response of the pipe that is given in the Cartesian coordinate system. The biggest advantage of this model is that it gives freedom to add different components to the system.

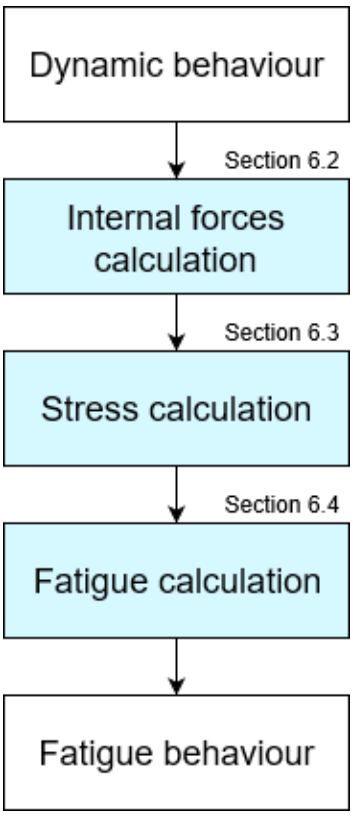

FIGURE 6.1: Overview additional MATLAB part

6.2 Internal forces calculations

The first step is to calculate the internal forces out of the dynamic behaviour of the freespan. The internal forces in the pipeline consist of the axial force, shear forces in y-direction and z-direction and the moments in y-direction and z-direction, as shown in figure 6.2. The shear force and moment in x-direction are not of interest.

A vector with these five internal forces could be calculated using formula 6.1. The pipeline's stiffness matrix and the tangent stiffness matrix are used, along with the deflections and rotations. The stiffness matrices are derived for the static deflection calculation. The deflections and rotations for each element of the pipeline are the output of the dynamic behaviour analysis. The dynamic behaviour analysis is in the time domain. Therefore, the internal forces can be generated for each time step.

$$Internal\ forces : F_{internal} = K_{element} \cdot U_{static} + T_{element} \cdot U_{dynamic} \tag{6.1}$$

$K_{element}$ is the stiffness matrix of the element
U_{static} is the vector for the static deflections and rotations
$T_{element}$ is the tangent stiffness matrix of the element
$U_{dynamic}$ is the vector for the dynamic deflections and rotations

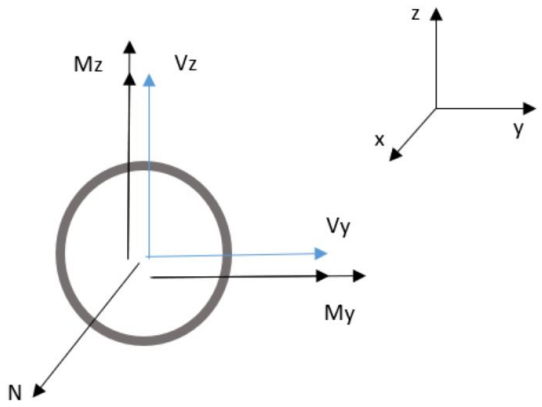

FIGURE 6.2: A schematic overview of the internal forces on a cross-section of the pipeline.

The $T_{element}$ that is introduced in formula 6.1 is the tangent stiffness matrix. This matrix describes the stiffness of the pipeline elements in response to small changes in configuration.

The internal forces are varying over the length of the pipeline. The model displays the moment and shear force variation in the moment and shear force diagrams of figure 6.3. The moment diagram shows that the highest moments are expected near the shoulders and in the mid-span of the freespan. This can be explained by the formula of the moment, as shown in formula 6.2. This formula contains the second derivative of the movement. This means that at the locations of the freespan where the curvature of the pipeline is the largest during the vibrations, the biggest moments occur. As seen in the envelope of the cross-flow vibration, this is near the shoulders and in the mid-span of the freespan.

$$Moment : M = EI\frac{d^2u}{dx^2} \tag{6.2}$$

E is the Young's modules of the pipeline's material $[Pa]$
I is the inertia of the pipeline element $[m^4]$
u is the deflection of the pipeline element $[m]$

6.3 Stress calculations

The next step is to calculate the stress in the freespan out of the internal forces and the pipeline dimensions. The normal stress cycles are dominant for the fatigue calculations. The shear stresses are not relevant for fatigue calculations in pipelines, because they are not significant if we consider a long structure with a relatively small diameter[29]. For the calculation of the normal stress cycles formula 6.3 is used.

Similar to the shear forces and the moments, the normal stress also varies over the length of the pipeline. The stress variation is displayed in the stress diagram of figure 6.4. The stress diagram shows that the highest stresses are expected near the mid-span.

$$Normal\ stress : \lambda_m = \frac{M_z}{I}\, r\, sin(\theta) + \frac{M_y}{I}\, r\, cos(\theta) + \frac{S_eff}{A_c} \tag{6.3}$$

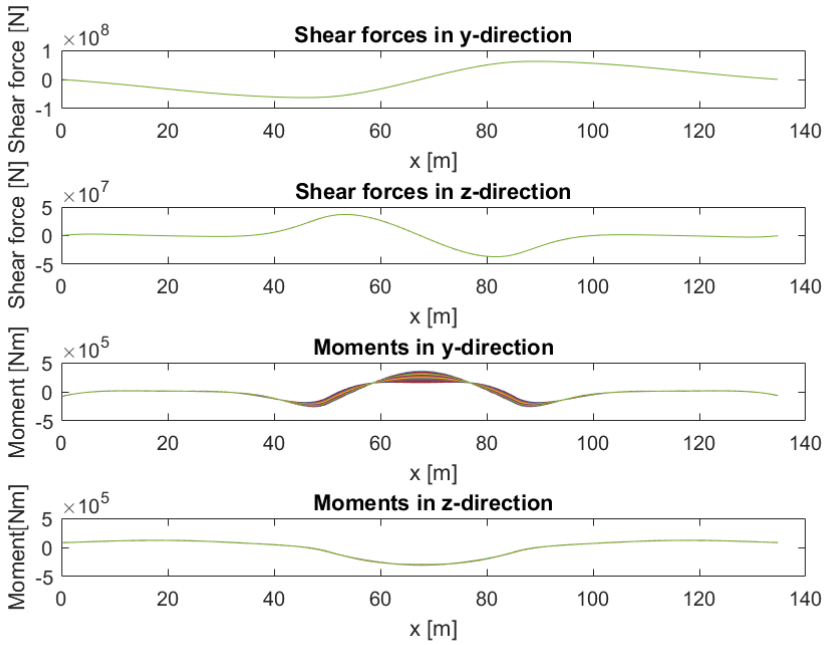

FIGURE 6.3: Shear force diagrams and moment diagrams of the freespan. The red dotted line indicates the shoulders of the freespan. The freespan is in between x=50 and x=85.

M_z	is the moment in z-direction $[Nm]$
r	is the outer radius of the pipeline $[m]$
θ	is the angle on the cross-section $[rad]$
M_y	is the moment in y-direction $[Nm]$
S_eff	is the effective axial force $[N]$
A_c	is the material surface of the pipeline cross-section $[m]$

Figure 6.6 display the stress cycles in the top of the middle node in the freespan. This graph shows the stress cycle amplitude and the stress cycle frequency.

6.3.1 Effective axial stiffness

The stiffness of the pipeline consists in the existing model of the material stiffness. However, the stiffness is a combination of the material stiffness and the geometric stiffness. The effective axial force adds this geometric stiffness to the model. The effective axial force represents the true steel wall axial force that takes the effect of internal and external pressures and the effect of temperature differences relative to pipeline laying into account. Formula 6.4 describes the effective axial force. It is difficult to include the exact real values in the calculation due to fluctuations of the variables.

$$Effective\ axial\ force: S_{eff} = H_{eff} - \Delta p_i A_i (1 - 2v) - A_c E \Delta T \alpha_e \tag{6.4}$$

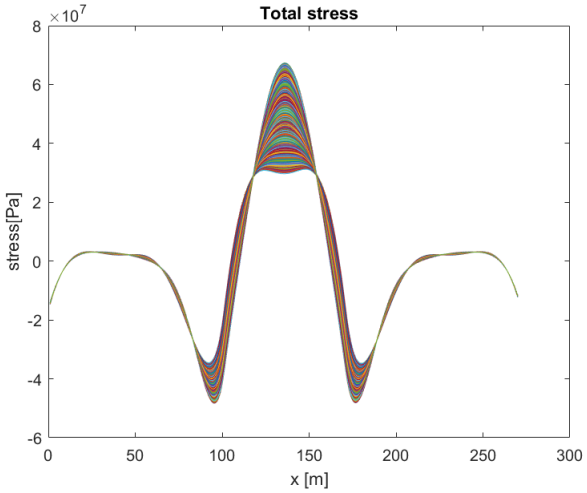

FIGURE 6.4: Stress distribution over the freespan. The freespan is in between x=100 and x=170.

H_{eff} is the effective lay tension $[N]$
Δp_i is the internal pressure difference relative to laying $[Pa]$
A_i is the internal cross section area of the pipe $[m^2]$
ν is the Poisson ratio $[-]$
ΔT is the temperature difference relative to laying $[^\circ C]$
α_e is the temperature expansion coefficient $[\frac{1}{^\circ C}]$

6.3.2 Critical locations

There are four points in the cross-section of a pipeline where the highest stresses are expected. These critical points are showed in figure 6.5. When the in-line VIV is dominant, the highest forces are expected at 0 and 180 degrees. When cross-flow VIV is dominant, the highest forces are expected at 90 and 270 degrees. Therefore, fatigue calculations will be done for these four points of the pipeline. The fatigue calculation that results in the highest fatigue damage is leading.

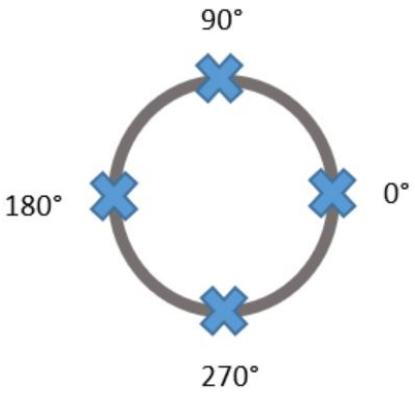

FIGURE 6.5: The critical points are showed in the cross-section of the pipeline.

6.4 Fatigue assessment

The last step is to calculate the fatigue damage in the material of the pipeline out of the stress cycles in the freespan.

6.4.1 Rainflow counting

The stress range of the stress cycles calculated in section 6.3 are varying over time. In order to calculate the fatigue damage, it is convenient to reduce this varying stress into bins of stress cycles with the same stress range. The Rainflow counting method [30] is widely used in the analysis of fatigue to create those bins.

Figure 6.6 displays the stress cycles determined in section 6.3. The Rainflow counting algorithm will determine the stress range for each cycle, as shown in figure 6.7. Thereafter, the Rainflow counting method will divide these cycles in different bins. The stress bins of figure 6.8 will be an input for the fatigue damage in calculations of section 6.4.2.

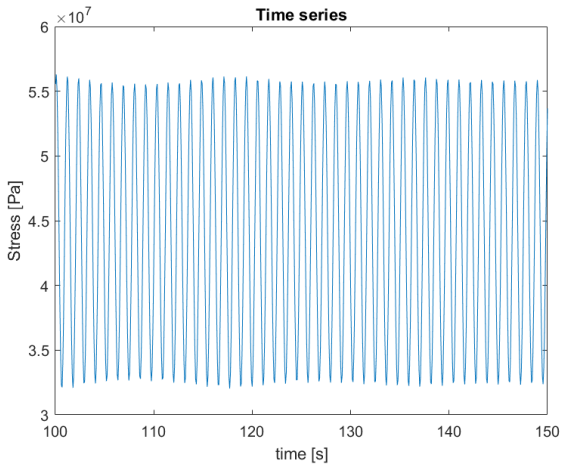

FIGURE 6.6: Time series of the stress fluctuation in the mid-span

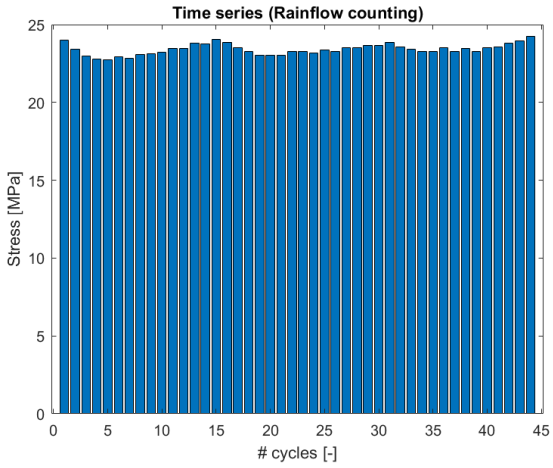

FIGURE 6.7: Time series (Rainflow counting) for the stress fluctuation in the mid-span

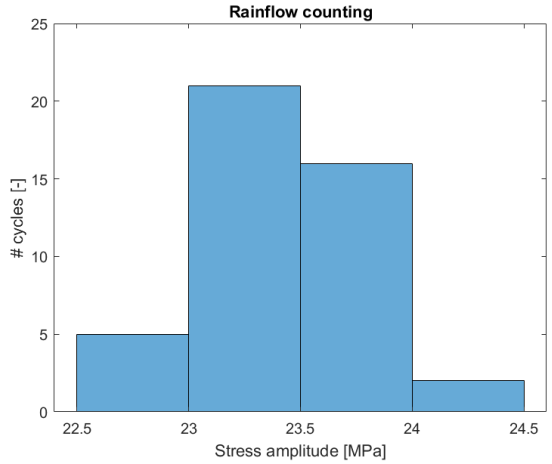

FIGURE 6.8: Rainflow counting for the stress cycles in the mid-span

6.4.2 Fatigue damage calculations

The fatigue damage due to VIV in the pipeline is first calculated for each stress bin separately and thereafter, the total fatigue damage is calculated based on the Palmgren-Miner Rule which applying the Miner summation [28]. Taken the following steps will result in the fatigue damage per stress bin:

1 Determine the total time that the freespan is subjected to VIV.

2 Determine the vibration frequency out of the time series of the mid-span.

3 Calculate the total number of stress cycles $[-]$ using the following formula:

$$Number\ of\ stress\ cycles : n = t_{tot} \cdot f_s \tag{6.5}$$

t_{tot} is the total time that the freespan is subjected to VIV $[s]$
f_v is the frequency of the VIV $[s^{-1}]$

4 Calculate the stress fluctuation per cycle

5 Determine the number of stress cycles that would result in pipeline failure. This number of cycles is determined from the SN-curves of the pipeline's material.

6 Calculate the fatigue damage $[-]$ using the following formula:

$$Fatigue\ damage : d = \frac{n}{n_f} \tag{6.6}$$

n_f is the number of stress cycles that would result in pipeline failure $[-]$

The time-domain numerical model will calculate the fatigue damage for each stress band and finally adding all the fatigue damages together to get the total fatigue damage in the pipeline. This total fatigue damage is used to calculate the fatigue lifetime, using formula 6.7.

$$Fatigue\ lifetime : T_{life} = \frac{1}{d} \tag{6.7}$$

6.5 Comparison between Fatfree and the time-domain numerical model for freespans

In this section, the outcomes of Fatfree will be compared with the outcomes of the time-domain numerical model for freespans. The comparison has been done for two case studies with different freespan specifications. Within these case studies, the outcome of different near-seabed velocities are compared. Both case studies consider hydrogen through a carbon steel pipeline.

6.5.1 Assumptions for the case studies

It is essential for the comparison between the time-domain numerical model and Fatfree to have the same input values. The following assumptions have been made to enable the comparison of the two programs:

- The effect of waves on the near-seabed current will not be taken into account.
- The current has a constant velocity.
- The direction of the current is perpendicular to the pipeline bearing.
- The pipeline is modelled without concrete layer and coating.
- The soil conditions are 'Sand-medium' based on DNV-RP-F105.

6.5.2 Partial safety factors for the case studies

The time-domain numerical model does not include safety factors in the calculations. It is not possible to perform Fatfree calculations without safety factors. The lowest safety factors are used for the Fatfree calculations in the case studies to minimise the influence of the safety factors in the comparison between both programs. The partial safety factors class "Very well defined" is displayed in table 4.1.

The safety factor η is used over the fatigue lifetime. To decrease the influence of the safety factors in the comparison between both programs, the safety factor η is not taken into account. This is done by multiplying the final fatigue lifetime by a factor of 2. Due to this, the Fatfree results become less conservative for both case studies.

6.5.3 Case study 1

Design basis of case study 1

Table 6.1 gives the characteristics of case study 1. The freespan length is chosen to be 30 meters because this is a realistic length for freespans in the southern North Sea. The gap height is 1 meter, such that the pipeline will not make contact with the seabed during vibrations.

Parameter	Value	Unit
Freespan characteristics		
Length	30	m
Gap between pipe and bottom	1	m
Pipeline dimensions		
Outer diameter	0,610	m
Steel wall thickness	0,02	m
Concrete thickness	0	m
Coating thickness	0	m
Constants		
Poisson's ratio	0,3	$-$
Temperature expansion coefficient	$1.17 \cdot 10^{-5}$	$1/^{\circ}C$
Young's modulus	$2.07 \cdot 10^{11}$	N/m^2
Functional loads		
Effective residual lay tension	0	N
internal pressure	110	bar
Temperature difference relative to installation	0	°C
Densities		
Steel density	18656	kg/m^3
Concrete density	3040	kg/m^3
Coating density	1200	kg/m^3
Content density	10	kg/m^3
Damping		
Modal structural damping	0.005	$-$
Hydrodynamic damping	0.000	$-$

TABLE 6.1: Parameter of case study 1

Results of case study 1

The fatigue lifetimes were tested in case study 1 for four different environmental loading cases. The results of the case study are displayed in tables 6.2, 6.3, 6.4 and 6.5. Comparisons showed that in Fatfree the VIV onset is reached at lower speeds than in the time-domain numerical model for freespans. This is the main reason that both programs have significantly different outcomes for the near-seabed current velocities of 1.2 m/s, 2.0 m/s and 2.8 m/s.

It can also be seen in the tables below that the stress ranges for Fatfree are much higher than in the time-domain numerical model. This has been investigated by comparing the stress range against the dimensionless deflection in the mid-span, as shown in figure 6.9. It can be seen that there is a linear relationship between the stress range and the dimensionless amplitude of vibration in the mid-span in Fatfree and that this relation has a non-linear relationship in the model. The significant difference between the stress range in Fatfree and the stress range in the model is mainly due to the non-linear soil behaviour in the model in comparison with the linear soil behaviour in Fatfree.

Case study 1

Parameter	Fatfree	Time-domain numerical model	Unit
Current velocity	1.2	1.2	m/s
Natural frequency	1.57	-	Hz
Reduced velocity	1.25	-	$-$
Az/D	0	0.002	$-$
Ay/D	0.048	0	$-$
CF stress range	0	0.87	MPa
IL stress range	74	0	MPa
Fatigue life	752	$3.9 \cdot 10^{16}$	$years$
Dominant VIV direction	IL	CF	

TABLE 6.2: Results case study 1 for V=1.2 m/s

Parameter	Fatfree	Time-domain numerical model	Unit
Current velocity	2.0	2.0	m/s
Natural frequency	1.57	-	Hz
Reduced velocity	2.09	-	$-$
Az/D	0.20	0.007	$-$
Ay/D	0.12	0.001	$-$
CF stress range	325	1.64	MPa
IL stress range	182	0.12	MPa
Fatigue life	$2.3 \cdot 10^{-4}$	$1.6 \cdot 10^{6}$	$years$
Dominant VIV direction	IL	CF	

TABLE 6.3: Results case study 1 for V=2.0 m/s

Parameter	Fatfree	Time-domain numerical model	Unit
Current velocity	2.8	2.8	m/s
Natural frequency	1.57	-	Hz
Reduced velocity	2.92	-	$-$
Az/D	0.42	0.018	$-$
Ay/D	0.11	0.0007	$-$
CF stress range	685	4.2	MPa
IL stress range	168	0.27	MPa
Fatigue life	$1.2 \cdot 10^{-5}$	$3.7 \cdot 10^{3}$	$years$
Dominant VIV direction	CF	CF	

TABLE 6.4: Results case study 1 for V=2.8 m/s

Parameter	Fatfree	Time-domain numerical model	Unit
Current velocity	3.6	3.6	m/s
Natural frequency	1.57	-	Hz
Reduced velocity	3.75	-	$-$
Az/D	0.65	0.6	$-$
Ay/D	0.10	0.08	$-$
CF stress range	1046	180	MPa
IL stress range	153	23	MPa
Fatigue life	$1.6 \cdot 10^{-6}$	$4.6 \cdot 10^{-3}$	$years$
Dominant VIV direction	CF	CF	

TABLE 6.5: Results case study 1 for V=3.6 m/s

VIV-onset for case study 1

The results of case study 1 for the different environment loading cases has shown that there is a significant difference in the VIV-onset between Fatfree and the time-domain numerical model. Table 6.6 displays the near-seabed current velocities where the VIV starts. The VIV-onset for the time-domain numerical model is determined for a minimum amplitude in the mid-span of 0.01 meter for in-line direction and 0.05 meter for cross-flow direction.

	Fatfree	Time-domain numerical model	Unit
Current velocity for IL VIV-onset	0,79	3,55	m/s
Current velocity for CF VIV-onset	1,6	3,4	m/s

TABLE 6.6: VIV onset for case study 1

The site-specific metocean data for the specified pipeline has a maximum near-seabed velocity due to currents and waves lower than 2 m/s. The time-domain numerical model gives a fatigue lifetime of 1600000 years for a constant velocity of 2 m/s. Therefore, there will be no significant fatigue damage if the pipeline is calculated with the time-domain numerical model.

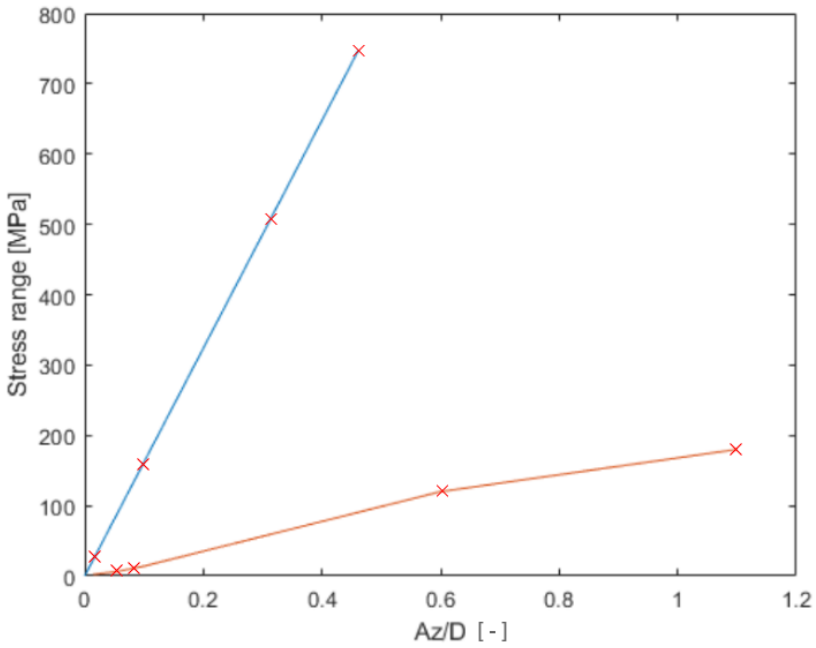

FIGURE 6.9: Cross-flow stress range as a function of the dimensionless amplitude in the mid-span. The blue line represents Fatfree and the orange line represents the time-domain numerical model.

6.5.4 Case study 2

Design basis for case study 2

The time-domain numerical model determines a VIV-onset for relativily high constant velocities for a freespan length of 30 meter in case study 1, which are unrealistic in the southern North Sea. To get a VIV-onset for lower velocities, case study 2 considers a freespan length of 60. If the freespan length increases, the natural frequency of the freespan decreases and the reduced velocity will increase. This results in VIV-onset for lower near-seabed velocities. The gap height is 4 meters, hence the pipeline will not make contact with the seabed during vibrations. Table 6.7 displays the characteristics of case study 2. Besides the constant current velocity and the gap height, all characteristics are the same as case study 1.

Parameter	**Value**	**Unit**
Freespan characteristics		
Length	60	m
Gap between pipe and bottom	4	m
Pipeline dimensions		
Outer diameter	0,610	m
Steel wall thickness	0,02	m
Concrete thickness	0	m
Coating thickness	0	m
Constants		
Poisson's ratio	0,3	$-$
Temperature expansion coefficient	$1.17 \cdot 10^{-5}$	$1/^{\circ}C$
Young's modulus	$2.07 \cdot 10^{11}$	N/m^2
Functional loads		
Effective residual lay tension	0	N
internal pressure	110	bar
Temperature difference relative to installation	0	°C
Densities		
Steel density	18656	kg/m^3
Concrete density	3040	kg/m^3
Coating density	1200	kg/m^3
Content density	10	kg/m^3
Damping		
Modal structural damping	0.005	$-$
Hydrodynamic damping	0.000	$-$

TABLE 6.7: Parameter of case study 2

Results of case study 2

The fatigue lives were tested in case study 2 for three different environmental loading cases. The results are given in tables 6.8, 6.9 and 6.10. As expected, the fatigue lives increase in comparison with case study 1 due to the increased freespan length. Comparison between case study 1 and case study 2 also show the stress ranges increase for longer freespan lengths if the vibration amplitudes are similar.

Parameter	**Fatfree**	**Time-domain numerical model**	**Unit**
Current velocity	1.0	1.0	m/s
Natural frequency	0.997	-	Hz
Reduced velocity	1.64	-	$-$
Az/D	0	0.02	$-$
Ay/D	0.091	0.001	$-$
CF stress range	0	5.5	MPa
IL stress range	50	0.21	MPa
Fatigue life	55	$6.6 \cdot 10^{2}$	$years$
Dominant VIV direction	IL	CF	

TABLE 6.8: Results case study 2 for V=1.0 m/s

Parameter	**Fatfree**	**Time-domain numerical model**	**Unit**
Current velocity	1.2	1.2	m/s
Natural frequency	0.997	-	Hz
Reduced velocity	1.97	-	$-$
Az/D	0.15	0.04	$-$
Ay/D	0.12	0.003	$-$
CF stress range	83	13	MPa
IL stress range	66	0.72	MPa
Fatigue life	$1.3 \cdot 10^{-2}$	12.4	$years$
Dominant VIV direction	CF	CF	

TABLE 6.9: Results case study 2 for V=1.2 m/s

Parameter	**Fatfree**	**Time-domain numerical model**	**Unit**
Current velocity	1.4	1.4	m/s
Natural frequency	0.997	-	Hz
Reduced velocity	2.30	-	$-$
Az/D	0.26	0.8	$-$
Ay/D	0.12	0.06	$-$
CF stress range	146	160	MPa
IL stress range	64	28	MPa
Fatigue life	$1.1 \cdot 10^{-3}$	$6.9 \cdot 10^{-3}$	$years$
Dominant VIV direction	CF	CF	

TABLE 6.10: Results case study 2 for V=1.4 m/s

6.5.5 Discussion of the results of the case studies

The results of the case studies show that there are significant differences between the outcomes of both programs. It is not possible to make a one-to-one comparison between the both programs because Fatfree uses a response model to determine the dynamic behaviour of a freespan and the time-domain numerical model uses a force model. However, there are some fundamental differences which lead to significant differences in results. These fundamental differences are discussed in this section.

Partial safety factors

The calculations in Fatfree are calibrated by laboratory tests and field measurements of offshore freespans. However, there is still uncertainty about the parameters predicting the VIV-response. To ensure that the target failure probability is achieved, according to industry standards, partial safety factors are introduced in the fatigue damage calculations. Therefore, they make the outcomes in Fatfree conservative. The time-domain numerical model does not include partial safety factors and is entirely developed based on physics and theory.

Soil behaviour

Another difference between both programs is a different approach for the soil behaviour. The time-domain numerical model uses a non-linear approach and Fatfree uses a more conservative linear approach.

In the time-domain numerical model, the soil-pipeline interactions are modelled with multiple springs and dash pots, as shown in figure 6.10. The resisting forces of the springs depending on the deflection of the pipeline. These forces will increase with increasing deflections of the pipeline nodes. The resisting forces of the dash pots are dependent on the velocities in which the pipeline nodes oscillate. The resistance of the dash pots will increase with increasing velocities of the nodes.

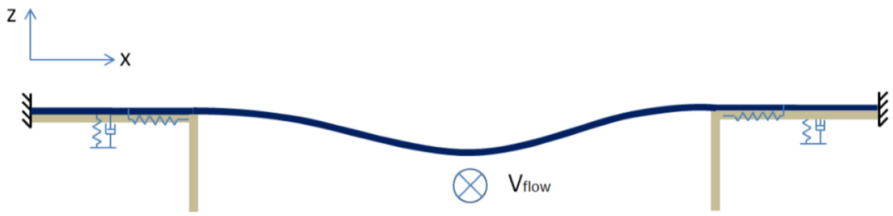

FIGURE 6.10: Model set-up [6]

The static position of the pipeline is determined with linear static springs that correspond to the type of soil and the weight of the pipeline. When the pipeline starts to oscillate, the soil behaves non-linearly. If the pipeline moves between static position and the seabed, the springs will behave the same as linear static springs for the determination of the static position. If the pipeline moves below the static position, the springs act as linear dynamic springs. The dynamic spring takes into account that the soil under the pipeline is compacted after installation compared to the soil before installation. The resistant force of the soil on the pipeline is shown in figure 6.11.

Fatfree takes linear soil behaviour into account instead of the non-linear soil behaviour in the time-domain numerical model. The non-linear soil behaviour approach will lead to lower

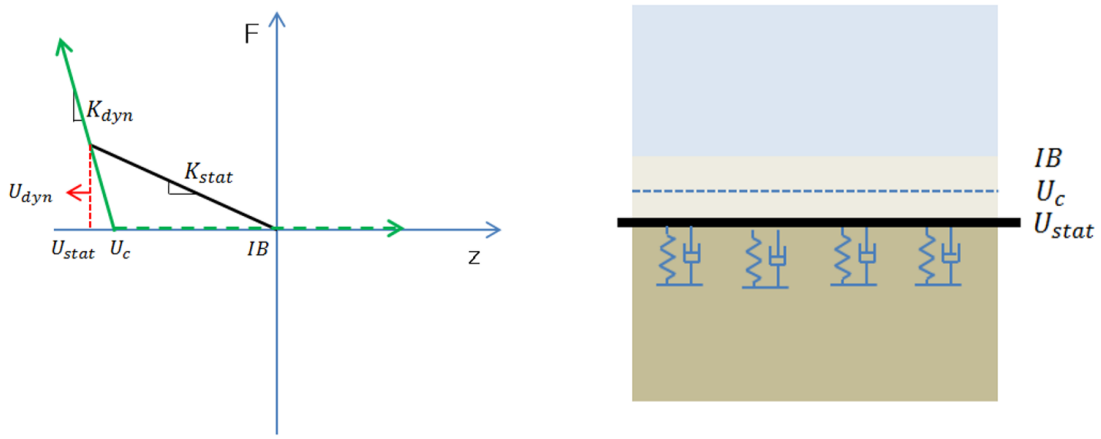

FIGURE 6.11: Left: The resistance force of a soil spring [6] Right: Pipeline position [6]

stresses in the pipeline. Therefore, the difference in results between Fatfree and the time-domain numerical model is partly explained by the difference in approach of the soil behaviour.

Vortex-induced vibrations onset

The results of the different case studies show that in Fatfree the Vortex-induced vibrations start at lower current velocities compared to the time-domain numerical model. When there is VIV for a particular current velocity in Fatfree and not in the time-domain numerical model, this will lead to significant differences in fatigue lifetime.

6.5.6 Stress distribution

In the time-domain numerical model, the highest stress fluctuation is determined in the mid-span for all cases. This is different in comparison with DNV-RP-F105 [28], which determines the highest stress fluctuation in the shoulders of the freespan for all case studies. The reason for this difference is the soil behaviour at the shoulders of the freespan. The non-linear soil approach decreases the stress at the freespan shoulders.

6.6 Conclusion

The time-domain numerical model for freespans is able to do fatigue damage calculations due to VIV for a constant near-seabed current. The model can determine the fatigue damage for each pipeline element. Therefore, the model can predict the fatigue damage distribution over the length of the pipeline. In the time-domain numerical model, the highest stress fluctuation is determined in the mid-span and Fatfree defines the highest stress for most cases near the shoulders of a freespan.

The time-domain numerical model gives a significantly higher fatigue lifetime compared to Fatfree. This is due to fundamental differences between the two programs, discussed in section 6.5.5. When the time-domain numerical model results are assumed to be correct, there will be no significant fatigue damage in the freespans of the specified pipeline.

Experiments are needed to validate the outcomes of the theoretical approach of the time-domain numerical model. An advantage of the model is that it is possible to easily introduce new components to the model, and therefore calibrate the calculations in the model with experimental results and new findings.

Chapter 7

Conclusions and recommendations

This chapter presents the conclusions of this research and recommendations for future research. The conclusions derived from the work conducted for this research are discussed in section 7.1. Thereafter, section 7.2 discusses the recommendations and remarks for future research.

7.1 Conclusions

Hydrogen transport through carbon steel pipelines leads to the penetration of atomic hydrogen into the materials the pipeline made of. The presence of atomic hydrogen in the material causes hydrogen embrittlement, which changes the material behaviour and degrades the steel performance. The literature study shows that the only effect of hydrogen embrittlement that endanger the feasibility of hydrogen transport through carbon steel pipelines is the change in fatigue behaviour. The fatigue SN-curves for carbon steel in a hydrogen environment is approached in this research to examine the change in fatigue behaviour of the carbon steel material. The SN-curve is approached with a conservative method that is based on the comparison between the fatigue behaviour of carbon steel material in a hydrogen environment and severe sour environments. The approached SN-curve has a fatigue life reduction which shows that the presence of atomic hydrogen in the pipeline's material has a significant influence on the fatigue behaviour of carbon steel pipelines.

The derived SN-curve for carbon steel material in a hydrogen environment is used to perform a fatigue analysis for the specified pipeline. This fatigue analysis outcomes show that the transition to hydrogen transport leads to an increase in fatigue damage rate for all the freespans in the pipeline. The number of freespans that do not fit the acceptance criteria of a maximum fatigue damage of 10 percent of the fatigue limit, increases with 50 percent in comparison with the transport of hydrocarbons. Therefore, the expected cost to mitigate the critical freespans will increase with the transition to hydrogen. However, this will not endanger the feasibility of hydrogen transport through the pipeline.

The fatigue analysis outcomes of the specified pipeline also show that the fatigue damage rate for critical freespans increases significantly. The probability of fatigue failure of these critical freespans will significantly increase in the time between successive pipeline inspections that are conducted ones in two years. This endangers the feasibility of hydrogen transport in the pipeline. Therefore, adjustments need to be made to avoid this increased probability of failure in the critical freespans.

An increase of the survey frequency, as well as preventive mitigation by pipeline trenching or rock dumping, are adjustments to the pipeline that can avoid the increased probability of failure due to the transition to hydrogen transport. Financial analysis shows that preventive mitigation by rock dumping of the pipeline sections that have a high probability on the

formation of critical freespans, has the lowest cost. Therefore, preventive mitigation by rock dumping is recommended for the specified pipeline to make it technical feasible to transport hydrogen through the pipeline.

The fatigue analysis for the specified pipeline has been done with the DNV freespan modelling program Fatfree that is based on the DNV Free Spanning Assessment Methodology. Fatfree uses a conservative approach for the fatigue damage calculation. The outcome of Fatfree is compared with a time-domain numerical model. This model is based on an existing model and is extended in this research to be able to perform fatigue damage calculations in the time-domain for each element over the length of the freespans. The time-domain numerical model gives significantly higher fatigue lives in comparison with Fatfree. This suggests that the methodology that is used for the fatigue analysis is too conservative. Under the assumption that the time-domain numerical model results are assumed to be correct, there will be no significant fatigue damage in all the freespans of the specified pipeline. However, there is still uncertainty about the influence of parameters predicting VIV in the model. Therefore, further calibration of the model is required to ensure that the model outcomes correspond with target failure probabilities regarding industry standards.

The time-domain numerical model shows that for freespans at sandy seabeds, the highest stress fluctuation in the pipeline due to VIV is expected in the mid-span. Therefore, the model expects the highest fatigue damage in the mid-span. The time-domain numerical model gives a different distribution of the stress over the length of the pipeline in comparison with the DNV Free Spanning Assessment Methodology. This methodology generates the highest expected stress fluctuation near the freespan shoulders.

The objective of this research was to assesses the technical feasibility of transporting hydrogen through offshore gas pipelines in the southern North Sea. The technical feasibility of hydrogen transport through a specific existing offshore gas pipeline in the southern North Sea has been assessed with a conservative approach, and it has been shown that this pipeline is technically suitable for the transport of hydrogen if the discussed adjustments are conducted. Compared to newly build pipelines for offshore hydrogen production, hydrogen transport through existing pipelines is an attractive option due to relatively low adjustment costs. This will make the offshore hydrogen production case more attractive in comparison with the onshore hydrogen production case.

7.2 Recommendations and remarks for future research

7.2.1 Recommendations regarding the approach of the SN-curve for carbon steel in hydrogen environment

The recommendations and remarks for the approach of the SN-curve for carbon steel in hydrogen environment are as follows:

- The derived SN-curve for carbon steel material in a hydrogen environment is based on available fatigue test data for carbon steel material in hydrogen and sour environments. The limited amount of fatigue data results in conservative assumptions in the SN-curve approach. Laboratory fatigue tests for carbon steel material in a hydrogen environment or a better explanation between H2S fatigue and H2 fatigue based on H-concentration in the steel are needed to determine the fatigue behaviour with higher certainty. A change in the SN-curve influences the outcomes of the fatigue analysis significantly.
- The addition of a relatively small amount of oxygen to the hydrogen could be effective to minimise the negative effect of hydrogen on the change of the material behaviour of the pipeline according to test data of Naturalhy [9]. Further research is needed to show the potential of the addition of a relatively small amount of oxygen in the pipeline.

7.2.2 Recommendations regarding the time-domain numerical model for freespans

The recommendations and remarks for the time-domain numerical model for freespans are as follows:

- The time-domain numerical model for freespans can conduct fatigue damage calculations in freespans for constant near-seabed currents. However, for pipelines that are located in shallow water, the waves will also influence the near-seabed current. Therefore, the model needs to be extended to incorporate the influence of waves to be able to do fatigue damage calculations for pipelines in shallow water.
- Fatfree is able to implement site-specific metocean data for the waves in $H_s - T_s$ and current diagrams, and for currents in U_c histograms. These diagrams include directional data with a given probability. In the time-domain numerical model, it is only possible to implement a constant near-seabed current. To conduct a complete fatigue analysis in the time-domain numerical model, the model needs to be able to implement these diagrams.
- The soil at the shoulders of the pipeline become weaker due to the vibrations of the pipeline. Therefore, the soil damping as a function of the vibration amplitude will change. This effect is not implemented in the time-domain numerical model, but can have a significant influence on the dynamic behaviour of the pipeline. Therefore, it is recommended to introduce this effect in the model.
- The Euler-Bernoulli beam of the time-domain numerical model uses a linear stress-strain relationship for the material. However, a non-linear stress-strain relationship for the material will give more realistic stresses. Therefore, it is recommend to introduce a non-linear stress-strain relationship for the material in the model.
- The outcomes of the time-domain numerical model are dependent on the parameters predicting the VIV-response. There is still uncertainty in the science community about the influence of these parameters on the system. Further calibration of each variable in

the model is required in such a way that the model outcomes will correspond to target failure probabilities.

Other important recommendations that were suggested by Morten Slingsby [6] to improve the time-domain numerical model are:

- To make the pipe-wake model a more universal model, the allowance for a change in cross-section along the length of the pipeline needs to be incorporated.
- The in-line amplitude is currently underestimated. Finding a wake-oscillator set-up in which both cross-flow and in-line amplitudes are estimated accurately would be an improvement on the model.

7.2.3 Recommendations regarding the future implementation of hydrogen transport in existing offshore pipeline in the southern North Sea

- This research has focused on the horizontal part of the pipeline on the seabed, as discussed in section 1.4. To introduce hydrogen as an energy carrier in future offshore energy projects, the scope of this research needs to be extended. It needs to be investigated if all components that are exposed to hydrogen in offshore hydrogen transport are able to withstand hydrogen, including compressors and valves.
- Gassco did a safety evaluation for hydrogen transport through existing offshore gas pipelines, in which a number of consequences of leakage or pipeline failure are elaborated [5]. A safety analysis for existing offshore pipelines needs to be done before the introduction of hydrogen transport in existing pipelines. It is recommended to quantify the consequences of all possible event and do an extensive safety analysis.
- This research has conducted a fatigue analysis for one specified pipeline. The other pipelines in the southern North Sea have other specification in terms of site-specific metocean data and freespan formation. Therefore, it is recommended to do a fatigue analysis for each individual pipeline that is selected to make the transition to hydrogen transport, and make a suitable adjustment plan.

List of Figures

List of Tables

Bibliography

[1] Van Wijk, A, "De Groene Waterstof-economie in Noord-Nederland," tech. rep.

[2] R. G. Derwent, "Hydrogen for heating: Atmospheric impacts," tech. rep., 2018.

[3] "Waterstof wint langzaam terrein."

[4] Patil, C S, "Offshore Wind to Hydrogen - Comparison of Onshore versus Offshore Hydrogen Production," tech. rep., 2018.

[5] Stromme, P A, "Presentation: Feasibility of hydrogen transport in existing ncs natural gas pipelines," 2017.

[6] Slingsby M, "Dynamic Interaction of Subsea Pipeline Spans due to Vortex-Induced Vibrations," tech. rep., 2015.

[7] Krom, A H M, Bakker, A, Koers, R W J, "Modelling hydrogen-induced cracking in steel using a coupled diffusion stress finite element analysis," tech. rep., 1997.

[8] Jones, D A, *Principles and prevention of corrosion*. 1996.

[9] Krom, A H M, "Naturalhy - State of the Art - Durability Integrity," tech. rep., 2005.

[10] DNV GL, "Verkenning waterstofinfrastructuur," tech. rep., 2017.

[11] Bermardo, C, Ang, S, "Presentation slides: SPEX GEP span Continuous Improvement Program."

[12] Blevins, R, *Flow-Induced Vibration*. 1990.

[13] Lienhard, J H, "Synopsis of lift, drag, and vortex frequency data for regid circular cilinders," tech. rep., 1966.

[14] B. U. M. Engineering, "Mechanics of Materials: Bending - Shear Stress."

[15] "Written communication: Email from Alfons Krom to Huub Hillen," 2019.

[16] Ashby, M, *Materials - Engineering, science, processing and design*.

[17] Lawrence, F V, "Presentation slides: Mechanisms of Fatigue Crack Initiation and Growth."

[18] Lazzarin, P, Tovo, R, Meneghetti, G, "Fatigue crack initiation and propagation phases near notches in metals with low notch sensitivity," tech. rep., 1997.

[19] Withagen, P M, *De invloed van de reksnelheid op de waterstof verbrossing van X-56 staal*. 1994.

[20] Ronevich, J A, "Presentation: Compatibility and suitability of existing steel pipelines for transport of hydrogen-natural gas blends," 2017.

[21] "Safebuck III JIP," tech. rep., 2013.

[22] Zhang, Y H, "TWI - Effect of Hydrogen Gas on the Fatigue Performance of Steel - Literature review ," tech. rep., 2011.

[23] Van Wortel, H, "Naturalhy - Preparing for the hydrogen economy by using the existing natural gas system as a catalyst," tech. rep., 2009.

[24] DNV GL, "Fatigue design of offshore steel structures, dnv-rp-c203," tech. rep., 2016.

[25] Matsunaga, H, "Slow strain rate tensile and fatigue properties of Cr-Mo and carbon steels in a 115 MPa hydrogen gas atmosphere," tech. rep., 2015.

[26] Yamabe, J, "Qualification of chromium-molybdenum steel based on the safety factor multiplier method in CHMC1-2014," tech. rep., 2015.

[27] "Written communication: Email from Jon Upton to Huub Hillen," 2018.

[28] D. GL, "Free spanning pipelines, dnv-rp-f105," tech. rep., 2006.

[29] B. U. M. Engineering, "Mechanics of Materials: Mechanics of Slender Structures."

[30] Downing, S D, Socie, D F, "Simple rainflow counting algoritm," tech. rep.

[31] Raaijmakers, T, "Morphodynamics of borssele wind farm zone wfs-iii, wfs-iv and wfs-v prediction of seabed level changes between 2015 and 2046.," tech. rep., 2016.

[32] Sequeiros, O E, Upton, J, Sznajder, D, Van der Werf, A, "Freespan mitigation study stage 1 report: Metocean, geotechnical, bedform migration analysis," tech. rep., 2018.

Appendix A

Hydrogen-damage mechanisms

A.1 Introduction

The transition to hydrogen transport through the specified pipeline will lead to changes in the material behaviour of the pipeline. This appendix gives an overview of these changes and their consequences for the feasibility of hydrogen transport through the specified pipeline . The change in fatigue behaviour is not explained in this appendix, because this subject is discussed in the main report.

It is complex to determine the effect of hydrogen on steel with laboratorial experiments, because the results depends on many input values and the atomic hydrogen is difficult to detect in the material. Therefore, theories have been developed to describe the effect of hydrogen on carbon steel in ambient temperatures [9]. However, none of these theories provide a complete explanation for hydrogen embrittlement, which suggests that hydrogen embrittlement can not be described with a single mechanism [19]. The two theories that are general accepted to describe hydrogen embrittlement are the Decohesion theory and the HELP theory [19].These theories are used in this appendix to describe the effect of hydrogen on the pipeline's material.

A.2 Hydrogen embrittlement

Hydrogen embrittlement is the degradation of material due to the presence of atomic hydrogen in the material. It effects the toughness and the ductility of the pipeline's material. The influence of hydrogen embrittlement on the steel has been shown with a comparison between tensile tests at room temperature in air and in hydrogen environment [9]. The outcome of tensile tests in air shows that the ductility is not dependent on the strain rate, and the outcome of tensile tests in hydrogen environment shows that the strain at fracture, measure of ductility, decreases if the strain rate decreases. Therefore, tests shows that the ductility is dependent on the strain rate in hydrogen environment.

A.3 Hydrogen induced cracking

A major form of hydrogen embrittlement is hydrogen induced cracking (HIC). HIC is a mechanical fracture caused by pressure development in metallurgical inhomogeneities (voids) in the material due to the recombination of atomic hydrogen into molecular hydrogen. This pressure can be sufficient to develop a internal crack. Therefore, HIC could effect the integrity

of the pipeline. The formation of internal cracks effects the fracture toughness and ductility of the pipeline's material.

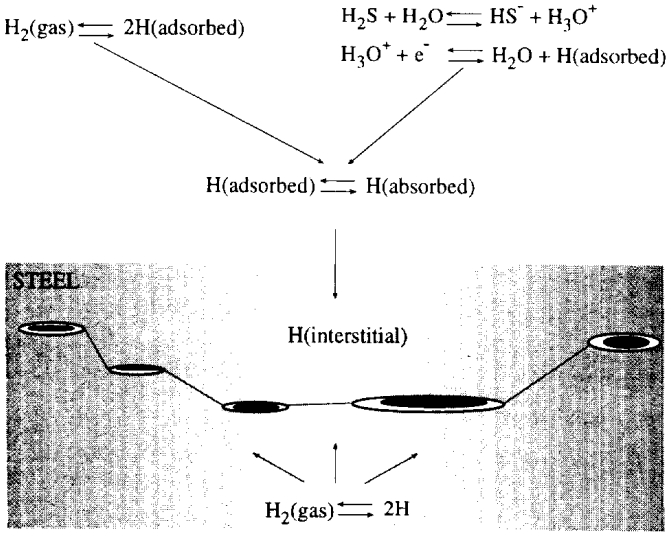

FIGURE A.1: Illustration of the penetration of atomic hydrogen in hydrogen environment [7].

A.3.1 Sour environments

HIC can occur in sour environments which contain hydrogen sulphide molecules. These hydrogen sulphide molecules can split into atomic hydrogen and atomic sulphide by an electrochemical reaction between steel and the environment. This reaction can be considered as a high pressure. Therefore, this reaction makes it possible that the concentration of atomic hydrogen in a void becomes extremely high. When the concentration of atomic hydrogen in a void is sufficient, atomic hydrogen will recombine to form molecular hydrogen in the gas phase. This leads to very high pressures in the void sufficient to rupture the inter atomic bonds [8]. The growth of this voids due to the high pressures is called blistering.

A.3.2 Hydrogen environment

Atomic hydrogen in a hydrogen environment is caused by the dissociation of molecular hydrogen. As shown in figure A.1, the atomic hydrogen could penetrate the pipeline's material and diffuse to the voids. A balance between the different traps in the material ensures that the potential pressure of the molecular hydrogen in the metallurgical inhomogeneities (voids) is dependent on the position of the metallurgical inhomogeneities. Therefore, the potential pressure in a void can not be higher than the hydrogen pressure inside or outside the pipeline, as shown in figure A.2.

The specified pipeline is made of carbon steel X65 material, and has a maximum operational pressure of 11 MPa for hydrogen transport. Therefore, the maximum pressure that can develop inside a void due to the recombination of atomic hydrogen to molecular hydrogen is 11 MPa. This potential pressure that can develop in voids due to the recombination of hydrogen atoms is insufficient to cause crack growth because the material bonds will be strong enough to prevent crack growth for this potential pressure. Therefore, the specified pipeline is HIC resistant.

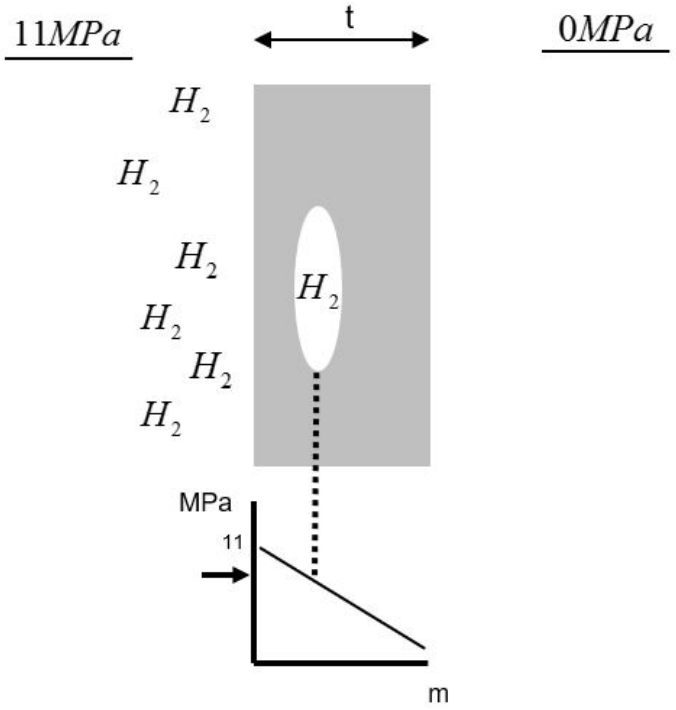

FIGURE A.2: Pressure balance of the pipeline's wall

A.4 Fracture resistance

The fracture resistance describes the ability of the material to resist fracture. Sandia National Institute has been investigating the fracture resistance of several carbon steel materials at various internal pressures [20]. The results of this research are displayed in figure A.3. The degradation of the fracture resistance increases with increasing operational pressure. It can be concluded from this graph that for an operational pressure of 11 MPa, the fracture resistance significantly decreases, but the fracture resistance will remain above the minimum fracture resistance from ASME B31.12 [].

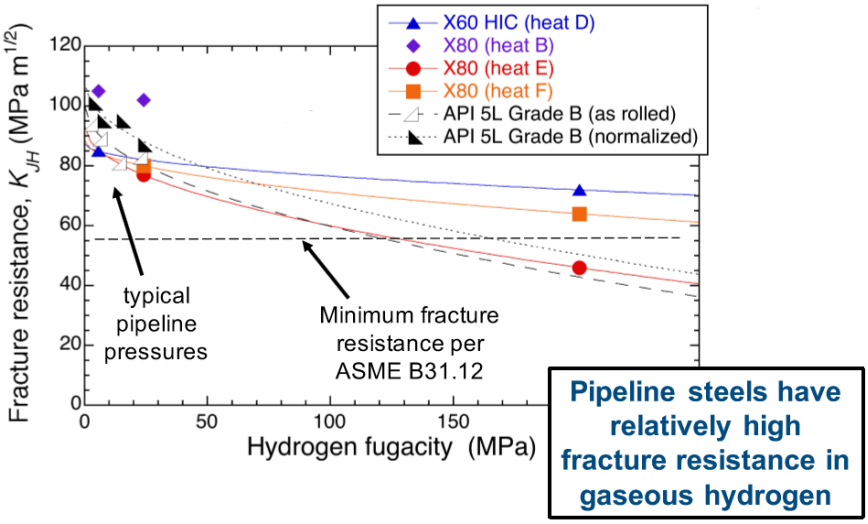

FIGURE A.3: Fracture resistance [20]

A.5 Prevention of hydrogen damage

Modification of the hydrogen environment could prevent hydrogen damage in the pipeline's material. An addition of a small amount of oxygen will lead to an oxidation layer at the internal surface of the pipeline. This layer could block hydrogen access to the steel [9]. It is also possible to prevent hydrogen damage by the selection of materials that are more resistant to hydrogen embrittlement.

Appendix B

Probability analysis for the formation of freespans

B.1 Introduction

This appendix provides a probability analysis for the formation of freespans, based on a sediment migration analysis [32] and historical freespan data. The pipeline is located in the southern North Sea which has a continually changing seabed topology. In areas with significant seabed migration, freespans could occur. Therefore, it is essential to understand the migration patterns thoroughly to identify which sections are prone to the formation of freespans. This seabed migration analysis assess the likelihood of the formation of future freespans in the different sections of the specified pipeline.

B.2 Morphodynamic seabed features

Morphodynamic seabed features are processes that by the influence of hydrodynamics, morphology and sediment transport can change the profile of the seabed. The four morphodynamic seabed features that take place in the southern North Sea are discussed in this section. These are the ripples, megaripples, sand waves and sandbanks. Figure B.1 shows some typical characteristics of these four features.

B.2.1 Ripples

Ripples are the smallest seabed features. Oscillating currents at the seabed form these ripples and their crest line can be straight or sinuous. Since ripples have a wave height in the order of centimetres, they have no significant influence on the seabed topology. Therefore, the ripples do not have a significant impact on the location of offshore pipelines.

B.2.2 Megaripples

Megaripples have a wave height in the order of decimetres, so therefore, these features have a more significant influence on the seabed topology than ripples. However, megaripples have a relative short wave length and such a high mobility that these features will quickly pass the offshore pipelines. Therefore, they have no significant impact on the location of freespans.

B.2.3 Sand waves

Sand waves are formed due to tidal currents and storm-induced waves and currents. Sand waves have a wave height in the order of meters, a wavelength in the order of 100s of meters and occur in water depths in the order of 20 - 40 meters. Therefore, sand waves have a significant effect on the seabed topology and can be a threat to pipelines because they produce significant freespans.

B.2.4 Sandbanks

Sandbanks are the biggest features with a wave height in the order of 10s or meters and wavelengths in the order of kilometres. However, these features are not a direct source of the formation of freespans because sandbanks are practically stationary in the lifespan of a pipeline.

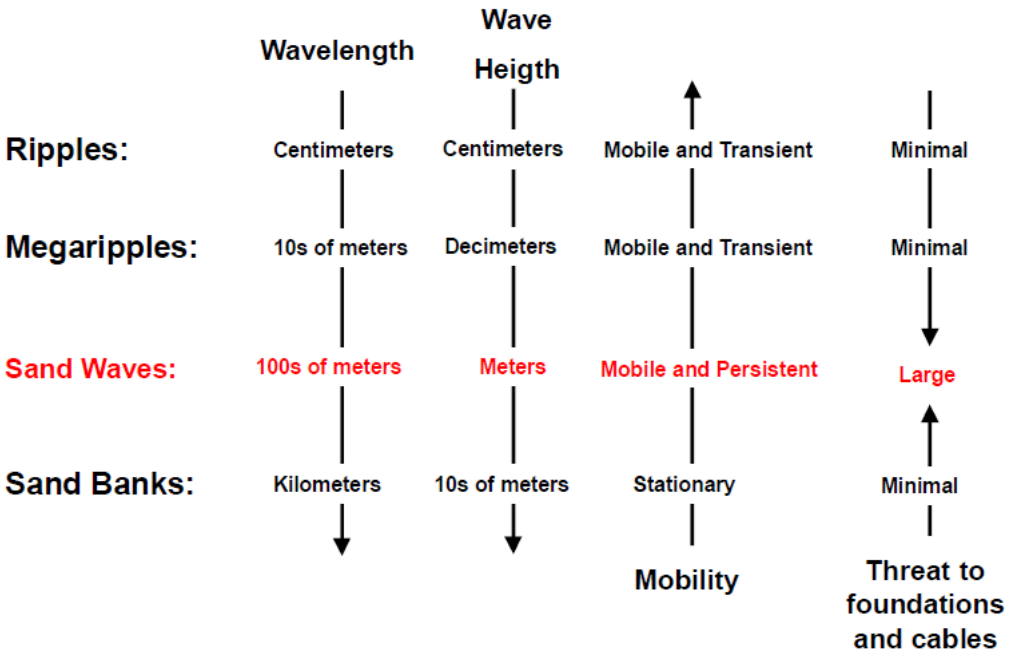

FIGURE B.1: Morphodynamic seabed features in the Southern North Sea and some typical characteristics [31]

B.3 Sediment transport

As explained in the previous section, only the sand waves have a significant impact on the location of the freespans. And, therefore, the sand waves are the main causer of VIV-induced fatigue. Sand waves are used as an indication of the predominant direction of sediment transport and have a speed in the order of several meters per year. Sandbanks are not directly a source of freespans, but the sandbanks have an influence on the direction of sediment transport by sand waves. The sand waves will turn around the sandbanks in a clockwise direction.

If sand waves cross a pipeline, they change the profile of the seabed. This could lead to the creation of freespans or a buried pipeline.

B.4 Future freespans in specified pipeline

It is plausible that in the future freespans will occur along the specified pipeline. Based on historical freespan data between 2000 and 2017 of IBIS and the sediment migration data, a probability analyses for every section of the pipeline is shown in the table B.1. Firstly, all the pipeline sections have received a rate between 1 and 3 for the 'Freespan occurred between 2000-2017' in with 1 means that no freespans are observed between 2000 and 2017, 2 means that a small amount of freespans has occurred in this section, and 3 means that several freespans have detected in this sections. Secondly, all the pipeline sections have received a rate between 1 and 3 for the 'Sand wave migration level' in with 1 means that there is a low amount of sand wave migration activity, 2 means that there is a medium amount of sand wave migration activity and 3 means that there is a large amount of sand wave migration activity. This probability values are composed of the two rates and give the likelihood that future freespans will occur in these sections.

Section	Freespans detected 2000-2017(1-3)	Seabed migration level(1-3)	Probability(1-3)
A	2	1	2
B	1	1	1
C	1	1	1
D	3	3	3
E	1	3	2
F	1	3	2
G	3	3	3
H	1	2	1
I	1	3	2
J	1	1	1
K	1	1	1

TABLE B.1: Probability analysis for freespans in the different sections of specified pipeline